

SANDIA REPORT

SAND2006-2244
Unlimited Release
Printed June 2006

Evaluation of Ceramic Papers and Tapes for Use as Separators in Thermal Batteries

Ronald A. Guidotti and Frederick W. Reinhardt

Prepared by
Sandia National Laboratories
Albuquerque, New Mexico 87185 and Livermore, California 94550

Sandia is a multiprogram laboratory operated by Sandia Corporation,
a Lockheed Martin Company, for the United States Department of Energy's
National Nuclear Security Administration under Contract DE-AC04-94AL85000.

Approved for public release; further dissemination unlimited.

Issued by Sandia National Laboratories, operated for the United States Department of Energy by Sandia Corporation.

NOTICE: This report was prepared as an account of work sponsored by an agency of the United States Government. Neither the United States Government, nor any agency thereof, nor any of their employees, nor any of their contractors, subcontractors, or their employees, make any warranty, express or implied, or assume any legal liability or responsibility for the accuracy, completeness, or usefulness of any information, apparatus, product, or process disclosed, or represent that its use would not infringe privately owned rights. Reference herein to any specific commercial product, process, or service by trade name, trademark, manufacturer, or otherwise, does not necessarily constitute or imply its endorsement, recommendation, or favoring by the United States Government, any agency thereof, or any of their contractors or subcontractors. The views and opinions expressed herein do not necessarily state or reflect those of the United States Government, any agency thereof, or any of their contractors.

Printed in the United States of America. This report has been reproduced directly from the best available copy.

Available to DOE and DOE contractors from
U.S. Department of Energy
Office of Scientific and Technical Information
P.O. Box 62
Oak Ridge, TN 37831

Telephone: (865) 576-8401
Facsimile: (865) 576-5728
E-Mail: reports@adonis.osti.gov
Online ordering: <http://www.osti.gov/bridge>

Available to the public from
U.S. Department of Commerce
National Technical Information Service
5285 Port Royal Rd.
Springfield, VA 22161

Telephone: (800) 553-6847
Facsimile: (703) 605-6900
E-Mail: orders@ntis.fedworld.gov
Online order: <http://www.ntis.gov/help/ordermethods.asp?loc=7-4-0#online>



Evaluation of Ceramic Papers and Tapes for Use as Separators in Thermal Batteries

Ronald A. Guidotti* and Frederick W. Reinhardt
Power Sources Development Department
Sandia National Laboratories
P.O. Box 5800
Albuquerque, NM 87185-0614

Abstract

Ceramic tapes and papers were evaluated for potential use as separators in high-temperature thermal batteries. The bulk of the tests involved fiberglass tape and borosilicate filter discs. Quartz (SiO_2) and zirconia (ZrO_2) materials were also examined to a limited extent. In addition, custom-prepared MgO-coated ceramic discs from Inventek Inc. were evaluated as separators. The tapes and paper discs were impregnated with LiCl-KCl eutectic or LiCl-LiBr-LiF electrolytes using three different techniques. Test discs were punched from the tapes and papers, impregnated with electrolyte and evaluated as separators in Li(Si)/FeS₂ single cells at 400° or 500°C at a steady-state current of 63 or 125 mA/cm². The performance of single cells containing these discs generally improved with increased electrolyte loading for most of the materials in the case of the LiCl-KCl eutectic. Better results were obtained with the paper filter discs than with the tapes. The best results with the paper discs were obtained with Whatman GF/A filter discs. Active lives for cells with these separators were about 85% of standard cells with pressed-powder separators. Good results were obtained in one battery test with the eutectic electrolyte. Mixed results were obtained with the LiCl-LiBr-LiF electrolyte under similar conditions. Higher loadings of electrolyte did not always translate into improved cell performance. Self-discharge reactions are believed responsible. The best overall results were obtained with the Inventek separators. Based on the results of this study, more work in this technology area is merited.

* Present address: Sierra Nevada Consulting, 1536 W. High Pointe Ct., Minden, NV 89432; e-mail: RonGuidotti@SierraNevadaConsulting.com

This page intentionally left blank.

Contents

Abstract.....	3
Contents.....	5
Figures.....	6
Tables.....	8
Introduction.....	9
Experimental Procedures.....	11
Materials.....	11
Electrochemical Testing.....	13
Single-Cell Tests.....	13
Battery Tests.....	14
Results and Discussion.....	14
Wettability Issues.....	14
Tests with LiCl-KCl Eutectic.....	15
Physical Characterization.....	15
Single-Cell Tests.....	16
Whatman Filter Discs.....	16
Inventek Separators.....	19
Commercialization.....	20
Battery Test.....	21
Tests with LiCl-LiBr-LiF Electrolyte.....	22
Single-Cell Tests.....	22
JPS Fiberglass Separator.....	22
GT#1 Fiberglass Separator.....	24
JPS Astroquartz Separator.....	24
Zircar ZYW-15 ZrO ₂ Tape.....	24
Fisher G-4 Filter Discs.....	25
Millipore Filter Discs.....	29
Whatman Filter Discs.....	33
Inventek Separator.....	45
Conclusions.....	48
References.....	49
Distribution.....	50

Figures

Figure 1.	Experimental Test Setup Used to Test Single Cell and Batteries.....	13
Figure 2.	Schematic Representation of the Wetting of a Solid by a Liquid Phase	15
Figure 3.	Surface of GF/C Filter Impregnated with Molten LiCl-KCl Eutectic (10- μ m Marker)	17
Figure 4.	Cross Section of Sample from Figure 2 (10- μ m Marker).....	17
Figure 5.	Performance at 400°C and 63 mA/cm ² Steady-State Current Density of Li(Si)/LiCl- KCl/FeS ₂ Single Cells made with Various Filter and Tape Separators.....	18
Figure 6.	Total Polarization at 400°C and 63 mA/cm ² Steady-State Current Density of Li(Si)/LiCl-KCl/FeS ₂ Single Cells made with Various Filter and Tape Separators ...	18
Figure 7.	Performance at 500°C and 125 mA/cm ² of Li(Si)/LiCl-KCl/FeS ₂ Single Cells using Inventek Ceramic Separator Discs.....	20
Figure 8.	Relative Performance at 125 mA/cm ² of 5-Cell Li(Si)/LiCl-KCl/FeS ₂ Batteries Activated at -54°C for Pressed-Powder and Ceramic-Fiber Separators.....	21
Figure 9.	Battery-Stack Temperature Profiles for Batteries of Figure 7	22
Figure 10.	Voltage Response at 500°C and 125 mA/cm ² Steady-State Current Density of Li(Si)/LiCl-LiBr-LiF/FeS ₂ Single Cells made with JPSFG Fiberglass-Tape Separator	23
Figure 11.	Total Polarization at 500°C and 125 mA/cm ² Steady-State Current Density of Li(Si)/LiCl-LiBr-LiF/FeS ₂ Single Cells made with JPSFG Fiberglass-Tape Separator	24
Figure 12.	Performance at 500°C and 125 mA/cm ² Steady-State Current Density of Li(Si)/LiCl- LiBr-LiF/FeS ₂ Single Cells made with Mutual Industries GT#1 Fiberglass-Tape Separator Dipped in Molten Electrolyte	25
Figure 13.	Voltage Response at 500°C and 125 mA/cm ² Steady-State Current Density of Li(Si)/LiCl-LiBr-LiF/FeS ₂ Single Cells made with JPS Astroquartz Quartz-Tape Separator	26
Figure 14.	Total Polarization at 500°C and 125 mA/cm ² Steady-State Current Density of Li(Si)/LiCl-LiBr-LiF/FeS ₂ Single Cells made with JPS Astroquartz Quartz-Tape Separator	26
Figure 15.	Performance at 500°C and 125 mA/cm ² Steady-State Current Density of Li(Si)/LiCl- LiBr-LiF/FeS ₂ Single Cells made with Zircar ZYW-15 ZrO ₂ Tape Separator	27
Figure 16.	Total Polarization at 500°C and 125 mA/cm ² Steady-State Current Density of Li(Si)/LiCl-LiBr-LiF/FeS ₂ Single Cells made with Zircar ZYW-15 ZrO ₂ Tape Separator	27
Figure 17.	Performance at 500°C and 125 mA/cm ² Steady-State Current Density of Li(Si)/LiCl- LiBr-LiF/FeS ₂ Single Cells made with Aqueous-Dipped Fisher G4 Filter	28
Figure 18.	Total Polarization at 500°C and 125 mA/cm ² Steady-State Current Density of Li(Si)/LiCl-LiBr-LiF/FeS ₂ Single Cells made with Aqueous-Dipped Fisher G4 Filter Separators.....	28
Figure 19.	Performance at 500°C and 125 mA/cm ² Steady-State Current Density of Li(Si)/LiCl- LiBr-LiF/FeS ₂ Single Cells made with Aqueous-Dipped Millipore APFA (1.5 μ m) Filter Separators	30

Figure 20. Total Polarization at 500°C and 125 mA/cm ² Steady-State Current Density of Li(Si)/LiCl-LiBr-LiF/FeS ₂ Single Cells made with Aqueous-Dipped Millipore APFA (1.5 μm) Filter Separators.....	30
Figure 21. Performance at 500°C and 125 mA/cm ² Steady-State Current Density of Li(Si)/LiCl-LiBr-LiF/FeS ₂ Single Cells made with Aqueous-Dipped Millipore APFC (1.2 μm) Filter Separators.....	31
Figure 22. Total Polarization at 500°C and 125 mA/cm ² Steady-State Current Density of Li(Si)/LiCl-LiBr-LiF/FeS ₂ Single Cells made with Aqueous-Dipped Millipore APFC (1.2 μm) Filter Separators.....	31
Figure 23. Performance at 500°C and 125 mA/cm ² Steady-State Current Density of Li(Si)/LiCl-LiBr-LiF/FeS ₂ Single Cells made with Aqueous-Dipped Millipore AP20 (0.8 μm min.) Filter Separators	32
Figure 24. Total Polarization at 500°C and 125 mA/cm ² Steady-State Current Density of Li(Si)/LiCl-LiBr-LiF/FeS ₂ Single Cells made with Aqueous-Dipped Millipore AP20 (0.8 μm min.) Filter Separators.....	32
Figure 25. Effect on the Performance at 500°C and 125 mA/cm ² Steady-State Current Density of Li(Si)/LiCl-LiBr-LiF/FeS ₂ Cells of the Median Pore Size of Millipore Filter Discs used as Separators and Loaded with Electrolyte by Aqueous Dipping	33
Figure 26. Performance at 500°C and 125 mA/cm ² Steady-State Current Density of Li(Si)/LiCl-LiBr-LiF/FeS ₂ Single Cells made with Aqueous-Dipped Whatman 934-AH (1.5 μm) Filter Separators.....	35
Figure 27. Total Polarization at 500°C and 125 mA/cm ² Steady-State Current Density of Li(Si)/LiCl-LiBr-LiF/FeS ₂ Single Cells made with Aqueous-Dipped Whatman 934-AH (1.5 mm) Filter Separators.....	35
Figure 28. Performance at 500°C and 125 mA/cm ² Steady-State Current Density of Li(Si)/LiCl-LiBr-LiF/FeS ₂ Single Cells made with Aqueous-Dipped Whatman TCLP (~0.7 mm) Filter Separators.....	36
Figure 29. Total Polarization at 500°C and 125 mA/cm ² Steady-State Current Density of Li(Si)/LiCl-LiBr-LiF/FeS ₂ Single Cells made with Aqueous-Dipped Whatman TCLP (~0.7 mm) Filter Separators	36
Figure 30. Performance at 500°C and 62 mA/cm ² Steady-State Current Density of Li(Si)/LiCl-LiBr-LiF/FeS ₂ Single Cells made with Whatman GF/C Treated Separators	37
Figure 31. Total Polarization at 500°C and 62 mA/cm ² Steady-State Current Density of Li(Si)/LiCl-LiBr-LiF/FeS ₂ Single Cells made with Whatman GF/C Treated Separators.....	37
Figure 32. Effect of Prewetting of Separator on Performance at 500°C and 62 mA/cm ² Steady-State Current Density of Li(Si)/LiCl-LiBr-LiF/FeS ₂ Single Cells made with Whatman GF/C Aqueous-Dipped Separators.....	38
Figure 33. Performance at 500°C and 125 mA/cm ² Steady-State Current Density of Li(Si)/LiCl-LiBr-LiF/FeS ₂ Single Cells made with Whatman GF/F Molten-Salt-Dipped Separators.....	39
Figure 34. Total Polarization at 500°C and 125 mA/cm ² Steady-State Current Density of Li(Si)/LiCl-LiBr-LiF/FeS ₂ Single Cells made with Whatman GF/F Molten-Salt-Dipped Separators.....	39
Figure 35. Effect of Electrolyte Loading of Separator of Li(Si)/LiCl-LiBr-LiF/FeS ₂ Cells made with GF/F Impregnated with Molten Electrolyte	40

Figure 36. Performance at 500°C and 125 mA/cm ² Steady-State Current Density of Li(Si)/LiCl-LiBr-LiF/FeS ₂ Single Cells made with Whatman GF/F Aqueous-Dipped Separators ..	41
Figure 37. Total Polarization at 500°C and 125 mA/cm ² Steady-State Current Density of Li(Si)/LiCl-LiBr-LiF/FeS ₂ Single Cells made with Whatman GF/F Aqueous-Dipped Separators.....	42
Figure 38. Comparison of Performance of Aqueous-Dipped and Molten-Salt-Dipped Separators at 500°C and 125 mA/cm ² Steady-State Current Density in Li(Si)/LiCl-LiBr-LiF/FeS ₂ Single Cells made with Whatman GF/F Separators	42
Figure 39. Performance at 500°C and 125 mA/cm ² Steady-State Current Density of Li(Si)/LiCl-LiBr-LiF/FeS ₂ Single Cells made with Whatman QMA Aqueous-Dipped Separators..	43
Figure 40. Total Polarization at 500°C and 125 mA/cm ² Steady-State Current Density of Li(Si)/LiCl-LiBr-LiF/FeS ₂ Single Cells made with Whatman QMA Aqueous-Dipped Separators.....	43
Figure 41. Performance at 500°C and 125 mA/cm ² Steady-State Current Density of Li(Si)/LiCl-LiBr-LiF/FeS ₂ Single Cells made with Whatman QMA Powder-Fusion Treated Separators.....	44
Figure 42. Total Polarization at 500°C and 125 mA/cm ² Steady-State Current Density of Li(Si)/LiCl-LiBr-LiF/FeS ₂ Single Cells made with Whatman QMA Powder-Fusion Treated Separators	44
Figure 43. Comparison of Performance of Aqueous-Dipped and Powder-Fusion-Treated Separators at 500°C and 125 mA/cm ² Steady-State Current Density in Li(Si)/LiCl-LiBr-LiF/FeS ₂ Single Cells made with Whatman QMA Separators	45
Figure 44. Performance at 500°C and 125 mA/cm ² Steady-State Current Density of Li(Si)/LiCl-LiBr-LiF/FeS ₂ Single Cells made with Inventek Ceramic-Disc Separators Treated by the Powder-Fusion Method	46
Figure 45. Total Polarization at 500°C and 125 mA/cm ² Steady-State Current Density of Li(Si)/LiCl-LiBr-LiF/FeS ₂ Single Cells made with Inventek Ceramic-Disc Separators Treated by the Powder-Fusion Method.....	46
Figure 46. Performance at 500°C and 125 mA/cm ² Steady-State Current Density of Li(Si)/LiCl-LiBr-LiF/FeS ₂ Single Cells made with Inventek Ceramic-Disc Separators Treated by the Aqueous-Dipping Method.....	47
Figure 47. Total Polarization at 500°C and 125 mA/cm ² Steady-State Current Density of Li(Si)/LiCl-LiBr-LiF/FeS ₂ Single Cells made with Inventek Ceramic-Disc Separators Treated by the Aqueous-Dipping Method	47

Tables

Table 1. Materials used in Initial Separator-Screening Study with LiCl-KCl Eutectic.....	12
Table 2. Materials used in Separator-Screening Study with LiCl-LiBr-LiF Electrolyte.....	12
Table 3. Relative Performance of LiSi/LiCl-KCl/FeS ₂ Cells at 400°C Under a Steady-State Load of 63 mA/cm ²	19
Table 4. Relative Performance of Li(Si)/LiCl-LiBr-LiF/FeS ₂ Cells at 500°C Under a Steady-State Load of 63 mA/cm ² using Whatman GF/C Filter Separators	38

Evaluation of Ceramic Papers and Tapes for Use as Separators in Thermal Batteries

INTRODUCTION

Thermally activated (“thermal”) batteries employ a Li-alloy anode [either Li(Si) or Li(Al)] and, most commonly, a cathode based on FeS₂ (pyrite). The separator is composed of a halide mixture, such as LiCl-KCl eutectic (melting point of 352°C), blended with MgO to immobilize the salt when it becomes molten upon activation by an internal pyrotechnic source. All the active thermal-cell components are prepared by cold pressing powder mixtures into pellets. The Li(Si)/FeS₂ couple has a nominal open-circuit voltage of 1.94 V at 500°C. Cells are stacked as required to obtain the desired voltage.

The increasingly higher demand for power and energy density of thermal batteries today requires reducing the thickness of piece parts as much as possible. The limit for thinner anodes and cathodes is dictated by the mass of electroactive material necessary to meet the intended application. The separator, on the other hand, could be reduced, since a thicker separator results in a higher IR drop in the battery. Pressing separator pellets to a thickness of 0.015” or greater is generally not a problem. However, pressing pellets that are less than 0.010” thick becomes increasingly more difficult as the diameter of the pellet is increased. Fabricating separators that are 3”–5” in diameter and <0.020” thick is extremely difficult—if not impossible—as they are extremely fragile and break easily during handling. In addition, it is not easy to spread a thin layer of powder into the pressing-die cavity. Consequently, there is a tendency for soft (low-density) spots or holes to form in such separator pellets. This results in a reduced pellet yield.

One way of mitigating this problem is to use a ceramic (e.g., AlN or MgO) monolith that can be impregnated with electrolyte. The electrical properties of AlN, for example, are very good for high-temperature battery applications.¹ This approach has been explored by workers at Northrop-Grumman and Argonne National Laboratory in rechargeable Li(Al)/LiCl-KCl/FeS₂ thermal cells for a proposed Army application.² This was an extension of similar work with ceramic separators performed at Argonne National Laboratory with Li(Al)/FeS and Li(Al)/FeS₂ batteries containing the same molten salt and other similar molten salts as part of its secondary-battery program for electric-vehicle applications—through the US Advanced Battery Consortium (USABC) program.^{3,4} Compatibility of AlN in high-temperature cells was examined by workers at General Motors as well.⁵

This sintered type of separator is prepared by conventional ceramic processing but suffers from certain physical constraints. A high porosity is necessary to minimize IR losses in the separator, but under such conditions, the separator tends to lack strength and crushes under the applied force needed during thermal battery construction. A low porosity imparts good strength, but results in a lower electrolyte loading that causes higher impedance. A similar approach has been used with LiAlO₂ separators for molten-carbonate fuel cells where the ceramic matrix was used as an electrolyte retainer.⁶

The use of ceramic felts has also been examined for high-temperature secondary cells. Argonne evaluated BN felt but found that it was not readily wet by the LiCl-KCl eutectic.⁴ General Motors also examined this material and experienced similar difficulties.⁷

A number of workers have examined the use of tapecasting to prepare separator discs. Various organic binders are blended with the separator powder to form a plastic material that can be calendared or rolled into sheets. Varta reported on the use of this technique for separator preparation for secondary high-temperature Li(Al)/FeS₂ batteries.^{8,9} The key factor for success with this approach is to use a binder that can be cleanly removed by thermal treatment without melting the electrolyte and forming objectionable pyrolysis products. For the LiCl-KCl-based separators, that means a binder that will volatilize completely at much less than 352°C. Polyisobutylene (PIB) meets this criterion, as it decomposes cleanly at 320°C. Pyrolysis to form elemental carbon would be unacceptable, as this would impart electronic conductivity to the separator. One disadvantage of tapecast separators is that it can be difficult to accurately control shrinkage and warpage during heat treatment. Thermal batteries require close dimensional control on the battery-stack components. There are also issues with strength and electrolyte retention with this method that need to be addressed further.

An alternate separator approach involves the use of glass- or ceramic-fiber separators that are impregnated with the molten electrolyte. In many cases, these are readily available commercially in thicknesses under 0.010". These materials are available in both a woven or paper (matte) form. An attractive feature of this approach is that the separator would provide additional insurance against intercell shorting because of the mechanical barrier that it would provide. With pressed-powder separators, there can be a tendency for material movement in very thin cells over prolonged (>2 h) discharge times. This could lead to bridging of the anode and cathode, initiating a potential thermal runaway. Use of such separators would obviate the need for expensive dies for large-diameter separators—the desired sizes could simply be punched from the impregnated materials—which could significantly reduce production costs for thermal batteries. It would be just as easy to punch a 3"-dia. disc as a 1"-dia. one. This concept is also attractive in that, in theory, it would allow the use of a prismatic design for thermal batteries. The standard right circular cylinder has certain volume constraints in terms of packaging for some applications.

While there have been some indications of their previous use, little has been reported in the literature in terms of the properties of such materials for separator use. Our initial work in this area previously reported showed promise.¹⁰ We undertook to extend this initial effort and conducted a systematic and comprehensive evaluation of this concept for our internal needs. A number of commercial fiberglass and quartz filter media and tapes were evaluated in the course of this work. The electrolyte is held in place in these materials in the same manner as with the powdered MgO separators, *i.e.*, by capillary action. Consequently, the porosity and pore-size distribution will determine the electrolyte loading and effective retention, as well as consequent separator resistance in a thermal battery environment.

The electrolytes used in the study were the LiCl-KCl eutectic (m.p. of 352°C) and the LiCl-LiBr-LiF, all-Li electrolyte (m.p. of 436°C). The loaded separator materials were incorporated into Li(Si)/FeS₂ single cells and tested galvanostatically at temperatures of 400° or 500°C at several current densities. The bulk of the tests were conducted at 500°C and 125 mA/cm² steady-state current density. These data were then compared to those for standard cells made with

conventional pressed-powder separators. A 5-cell battery test was also conducted. The results of these studies will be presented in this report and problem areas associated with this technology will be discussed.

EXPERIMENTAL PROCEDURES

Materials

Single cells, 1.25" in diameter, were fabricated using flooded anodes consisting of 75% of 44% Li/56%^a Si alloy and 25% electrolyte (0.93-g, 0.042" thick). The Li(Si) alloy was obtained from Eagle-Picher Industries. The LiCl-KCl eutectic electrolyte was made in house by fusion of reagent grade LiCl and KCl in the appropriate amounts at 600°C for three hours in a quartz crucible in a dry room maintained at <3% relative humidity. The all-Li, LiCl-LiBr-LiF electrolyte was prepared in the same manner. The electrolytes were pulverized and blended with 35% MgO [Merck (now Calgon) Maglite 'S']. The LiCl-KCl-based separator mix was fused overnight at 400°C in the dry room to prepare the control separator material, which was then pelletized (1 g, 0.027" thick). A temperature of 500°C was used for the all-Li separator mix. An unfused, lithiated cathode that had the composition 73.5% FeS₂/25% separator/1.5% Li₂O (1.03 g, 0.018" thick) was used for all tests.

The separator materials that were evaluated with the LiCl-KCl eutectic in the preliminary investigations are listed in Table 1, along with the loading of electrolyte per 1.25"-dia. disc. Comparable data are provided in Table 2 for materials tested with the LiCl-LiBr-LiF electrolyte. The bulk of these filter materials were borosilicate glasses rated to 500°C. The tapes and Zircar samples were woven, while the other samples were in a paper (matte) form. The custom-fabricated material from Inventek, Inc. (New Lenox, IL) is believed to be a sintered aluminosilicate ceramic material coated with MgO. The electrolyte loading varied considerably for the various materials due to differences in thickness, open porosity, and wettability.

The sample discs were loaded with electrolyte by three different techniques. In the first method, the sample discs were immersed in a bath of the molten electrolyte at 450°C for the LiCl-KCl eutectic and 500°C for the all-Li electrolyte for 10 – 20 minutes. Some materials wetted readily (*e.g.*, Whatman GF/F), while the others required contact times up to 20 minutes, to ensure complete wetting. After impregnation in the molten eutectic, the materials were placed on a quartz plate and heated at 400°C for 15 minutes in an oven, followed by removal and cooling; a temperature of 500°C was used in the case of the all-Li electrolyte. This was done to ensure flat samples for the subsequent punching of the 1.25"-dia. test discs.

^a Unless noted otherwise, all compositions are reported in weight percent.

Table 1. Materials used in Initial Separator-Screening Study with LiCl-KCl Eutectic.*

<u>Product</u>	<u>Manufacturer</u>	<u>Nominal Thickness, in</u>	<u>Nominal Pore Size, μm</u>	<u>Electrolyte Loading, g[#]</u>
GF/A filter	Whatman	0.010	1.6	0.273-0.395
GF/C filter	Whatman	0.010	1.2	0.430-0.517
GF/F filter	Whatman	0.017	0.7	0.592-0.610
GT#1 (FG) tape	Mutual Industries	0.005	Unknown	0.183
Custom discs (1DR)	Inventek	0.0289 – 0.0362	Unknown	0.70–01.45

* All materials borosilicate glass, except where noted otherwise.

Loading per 1.25"-dia. test disc after immersion in molten salt.

Table 2. Materials used in Separator-Screening Study with LiCl-LiBr-LiF Electrolyte*.

<u>Product</u>	<u>Manufacturer</u>	<u>Nominal Thickness, in</u>	<u>Nominal Pore Size, μm</u>	<u>Electrolyte Loading, g[#]</u>
Unknown tape	JPS Glass	0.0047	Unknown	0.180 – 0.220
GT#1 (FG) tape	Mutual Industries	0.005	Unknown	0.121 – 0.158
Astroquartz (SiO ₂) tape	JPS Glass	0.0054	Unknown	0.183 – 0.253
ZYW-15 (ZrO ₂)	Zircar	0.010	87% porous	0.196 – 0.398
GF/C	Whatman	0.010	1.2	0.117 – 0.259
GF/F	Whatman	0.017	0.7	0.123 – 0.755
TCLP	Whatman	0.017	0.6 – 0.8	0.130 – 0.536
934-AH	Whatman	0.013	1.5	0.131 – 0.546
QMA (SiO ₂)	Whatman	0.016	Fine (<0.3)	0.140 – 0.744
G4	Fisher	0.011	Unknown	0.0909 – 0.440
APFA	Millipore	0.0197 – 0.0248	1.5	0.162 – 0.472
APFC	Millipore	0.0126 – 0.0142	1.2	0.130 – 0.505
AP20	Millipore	0.0118 – 0.0157	0.8 – 8.0	0.157 – 0.179
Custom discs (1DR)	Inventek	0.0289 – 0.0362	Unknown	0.380 – 0.550

* All materials borosilicate glass, except where noted otherwise.

Loading per 1.25"-dia. test disc after immersion in molten salt.

In the second method, the sample discs were immersed in a saturated aqueous solution of the electrolyte and then vacuum dried at 80° – 100°C for several hours to remove residual water. In a modification of this technique, the discs were first immersed in deionized water prior to immersion in the salt solution (so-called “prewetting”). This aided in wetting but reduced the overall salt loading that was achieved.

The last impregnation technique involved placing preweighed amounts of powdered electrolyte on top of the sample discs that were then placed on quartz plates. These were then heated in an oven at either 400°C (for the LiCl-KCl eutectic) or 500°C (for the all-Li electrolyte) for 15 – 20 minutes, to allow the molten electrolyte to wet, penetrate, and disperse throughout the sample.

All salt, separator, and sample preparations were conducted in a dry room maintained at <3% relative humidity.

Electrochemical Testing

Single-Cell Tests

A HP6060B, a 60-A/300-W programmable electronic load, was used for the initial single-cell screening tests. Two HP3458A high-speed DVMs were incorporated—one for the cell/battery voltage and the other for the current—to allow digitization of the pulses applied during discharge. A schematic of the test setup is shown in Figure 1. Considerable time was spent developing the necessary software to allow testing of the single cells under a wide range of discharge profiles. The timing and triggering of the load and DVMs were critical for complete capture of the pulse response.

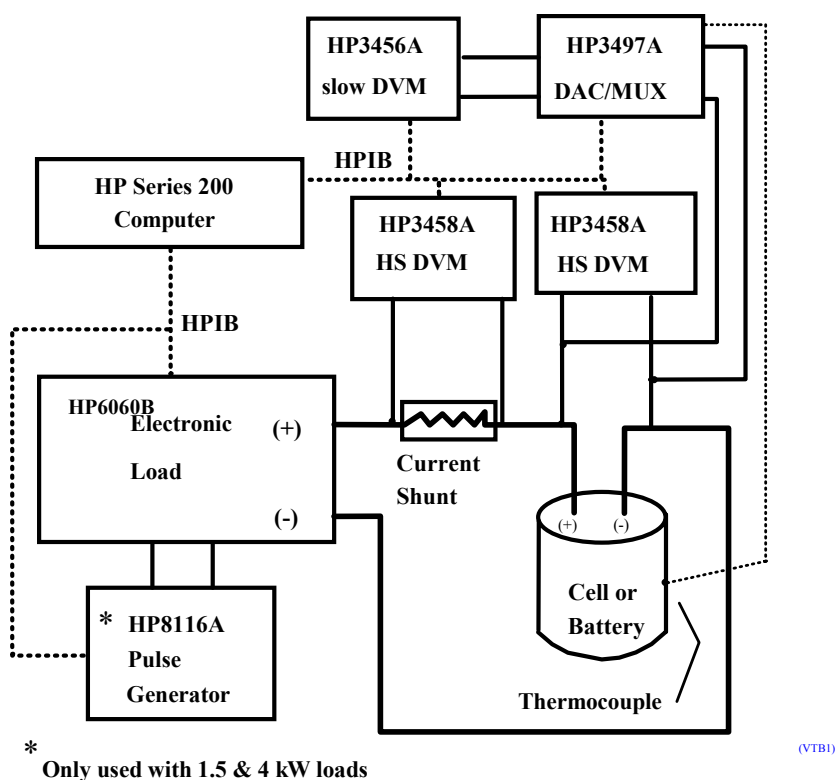


Figure 1. Experimental Test Setup Used to Test Single Cells and Batteries.

Single cells were tested between heated platens at either 400° or 500°C using an applied pressure of 8.0 psig. They were discharged galvanostatically under computer control in a glovebox under an atmosphere of high-purity argon (<1 ppm each of O₂ and H₂O). The cells were discharged to a cutoff voltage of 1.25 V at a steady-state current of either 0.5 A (~63 mA/cm²) or 1.0 A (125 mA/cm²). The current was doubled for 1 s every 60 s to allow overall cell polarization to be monitored as a function of depth of discharge. Each test was repeated at least once.

Battery Tests

The same test setup used for single-cell tests was used for the 5-cell battery tests. Each battery contained a type-K thermocouple in the stack in the cell furthest away from the header end. The battery stacks were wrapped with four wraps of 0.080"-thick Fiberfrax® blanket, with ¼"-thick Min-K® pads on the ends. The batteries were activated at -54°C and were discharged to a cutoff voltage of 6.25 V (1.25 V/cell).

RESULTS AND DISCUSSION

Wettability Issues

The wettability of the surface by the electrolyte or solution has a dramatic effect on the ease of penetration into the fabric or pores of a mat, fabric, or powder. For good wetting, the contact angle must be low (*e.g.*, <90 degrees). Poor wettability will result in a low electrolyte loading. The three-phase region of gas, solid, and liquid is determined by the relative energies involved, as shown in Figure 2.

This will determine the final contact angle of the liquid on the solid.^{12,13} In the case of the pressed-powder separator materials (MgO) or the various filter or woven materials, the contact angle will be that of the molten salt. The solid-vapor surface tension, γ_{SV} , reflects the interaction of the solid and gas phases. The liquid-solid surface tension, γ_{LS} , reflects the interaction of the solid and liquid phases. The liquid-vapor surface tension, γ_{LV} , reflects the interactions of the liquid and vapor phases. The net interaction is defined by Young's equation:

$$\gamma_{LV} \cos(\phi) = \gamma_{SV} - \gamma_{SL} \quad [1]$$

In the case of separators for thermal batteries, the factors that are relevant are:

- composition of the separator material (including impurities)
- composition of the molten salt
- composition of the atmosphere surrounding the sample
- surface tension of the molten salt
- temperature
- pressure (this is important in a real battery)

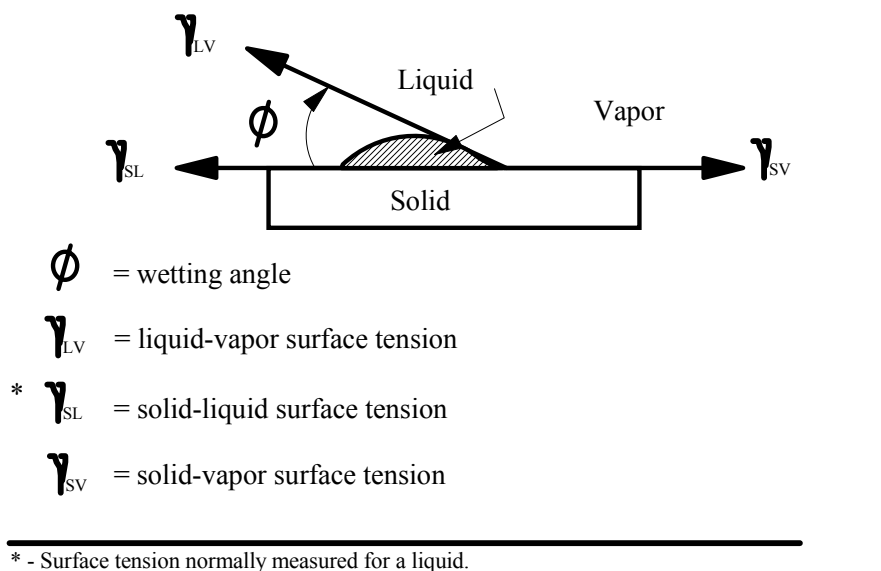


Figure 2. Schematic Representation of the Wetting of a Solid by a Liquid Phase.

The first factor affects the γ_{SV} and γ_{SL} terms in eqn. 1; the second factor affects the γ_{LV} term and the third factor affects the γ_{LV} and γ_{SV} terms. The surface tension (fourth factor) and viscosity of the molten salt are dependent on temperature (the fifth factor), typically being less at the higher temperatures.

These factors influence how the various separator materials will interact with various molten salts. It also explains why some MgO materials work quite well for immobilization of a molten-salt phase while others totally fail. The overall distribution of electrolyte in a cell will be affected by the amount of electrolyte in the separator and the relative wettability of the cell components by the electrolyte. This will determine the ultimate distribution of electrolyte throughout the cell during discharge. These interactions can be strongly influenced by the composition of the molten salt and temperature, as well as the applied pressure to the cell during discharge.

Ideally, one would like to be able to model the ideal monolithic separator to ascertain the optimum pore-size distribution for use in a thermal battery. Since this was not possible, it was necessary to empirically evaluate each of the candidate materials under simulated thermal battery discharge conditions.

Tests with LiCl-KCl Eutectic

Physical Characterization

The electrolyte loadings for the various samples were measured prior to the assembly of the separator discs into single cells. As seen in the data of Table 1, the filter discs with the smallest nominal pore size had the highest electrolyte loading. If the electrolyte loading is insufficient, the separator will be starved which will result in a greater tortuosity with a corresponding higher internal cell impedance during discharge. Similarly, excessive loading of electrolyte can lead to electrolyte leakage during discharge which can cause parasitic losses between cells in a battery stack. Also, when the sample is removed from the oven after impregnation with electrolyte,

greater stress can result during electrolyte freezing if there is excess electrolyte present. [If the samples are cooled too quickly after electrolyte loading, warpage can sometimes occur, which makes the samples of little or no use for test purposes. In addition, the sample can crack, which destroys the integrity of the material.]

A number of representative impregnated samples were taken for examination by scanning electron microscopy. Figure 3 shows a surface profile for a sample of GF/C impregnated with electrolyte. The wetting was fairly uniform and complete, as seen in Figure 4 for a photomicrograph of this sample after cross sectioning.

The mechanical properties of the impregnated materials are also important. If the impregnated material is too brittle, it can break during punching. This was not commonly observed with the tape materials as the fibers are much longer than those in the disc form and act as reinforcing material to increase strength.

Single-Cell Tests

Whatman Filter Discs – Typical performance at 400°C for Li(Si)/LiCl-KCl/FeS₂ single cells made with the various Whatman GF/x molten-salt-impregnated filter discs and a fiberglass tape are shown in Figures 5 and 6 for a steady-state current density of 62 mA/cm². Data for cells built with a standard pressed-powder separator are also shown for comparison. A temperature of 400°C was chosen for the initial characterization tests as any concentration gradients originating at the Li(Si) anode will be accentuated. At this temperature, the cell is only ~50°C above the melting point of the electrolyte. Any strong concentration gradients will cause the electrolyte composition in the separator to quickly deviate from the eutectic composition at the anode-separator interface, giving rise to LiCl precipitation and an attendant increase in the cell impedance.

The standard cell and the cells with the GF/C and GF/F separators showed a voltage transition near 0.4 eq. Li/mol FeS₂ (Figure 5). This voltage transition was not evident, however, for the cell with the GF/A separator, which had the highest voltage to a capacity of 1.2 eq. Li/mol FeS₂ (on the lower-voltage plateau).¹ The corresponding cell-polarization data showed maxima occurring during the voltage transitions (Figure 6). The pulse response of the cell with the GF/A separator showed essentially all of the polarization to be ohmic, whereas some concentration polarization was evident for the standard cell under the same conditions. The cell with the fiberglass-tape separator showed good initial performance, but the cell voltage rapidly dropped off near 0.5 eq. Li/mol FeS₂ as the cell impedance rapidly rose (Figure 6). In general, the overall cell polarization (impedances) for cells with the filter and tape separators were comparable or lower than those for the control cells with pressed-powder separators. The overall cell polarization was the lowest for the cell with the GF/A separator, which also had the second lowest loading of electrolyte.

¹ Complementary tests with a reference electrode showed that these transitions are associated with the cathode during formation of the first discharge phase, Li₃Fe₂S₄.

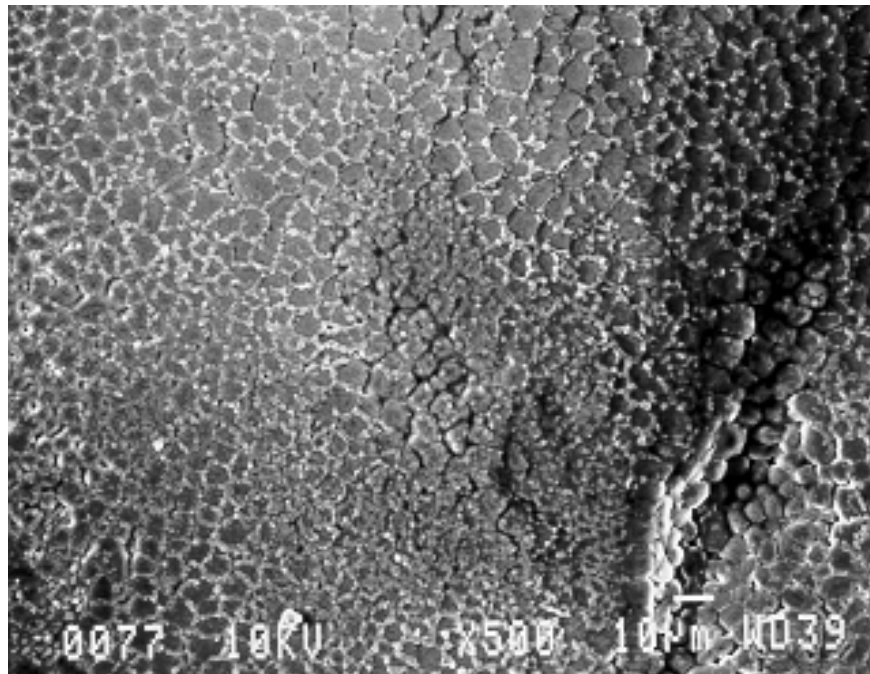


Figure 3. Surface of GF/C Filter Impregnated with Molten LiCl-KCl Eutectic (10- μ m Marker).

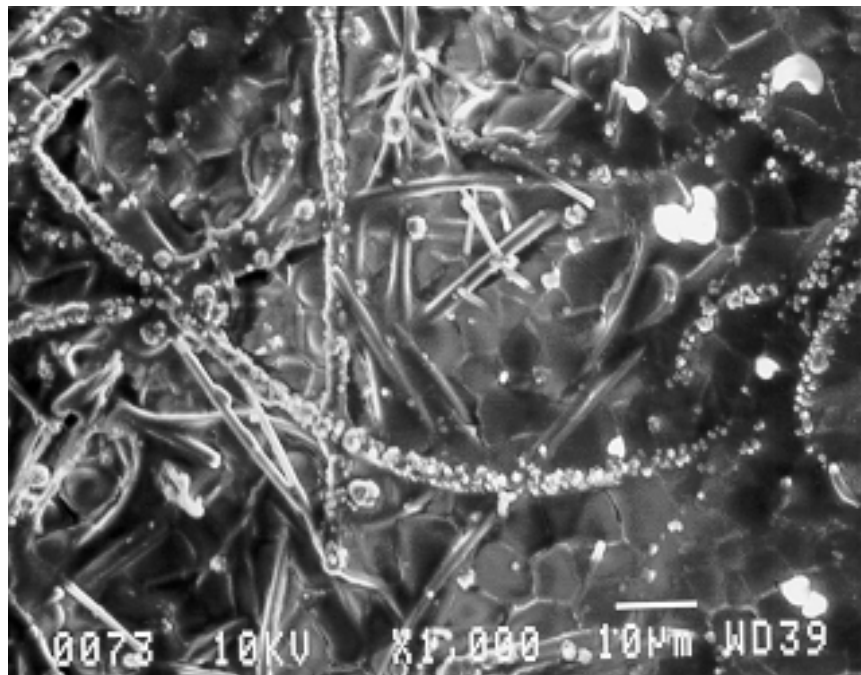
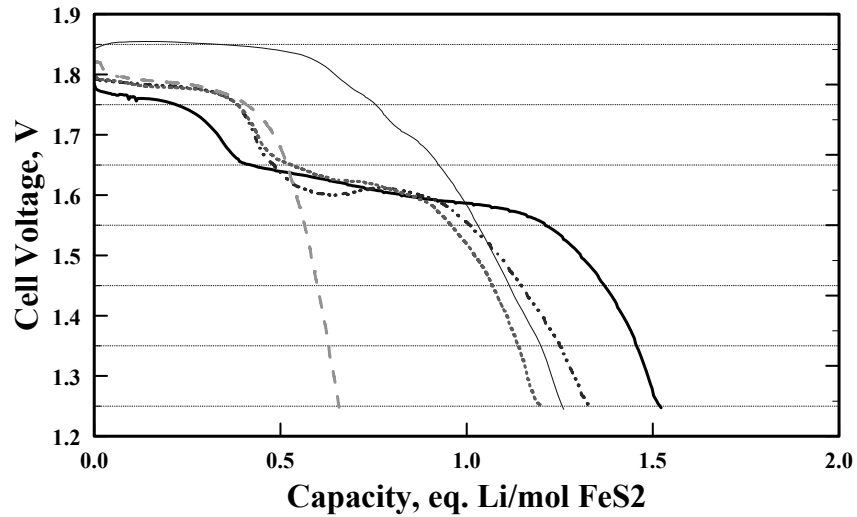


Figure 4. Cross Section of Sample from Figure 3 (10- μ m Marker).

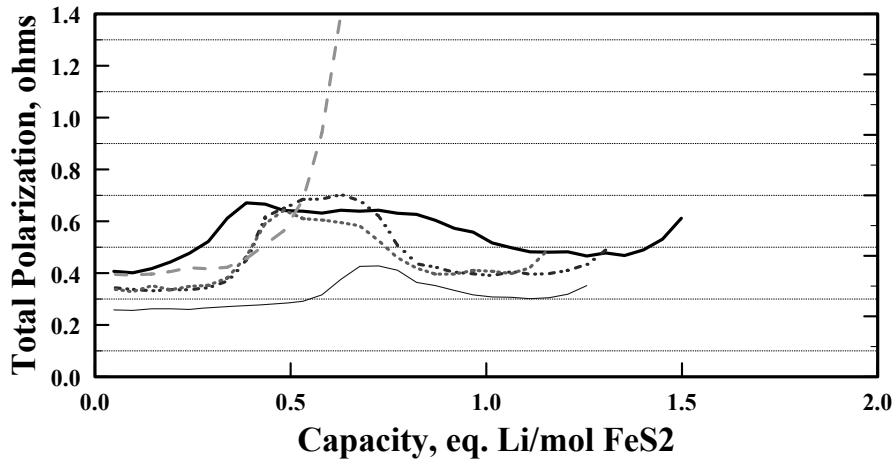


Pressed Powder (0.670g E)	GFA (0.395g E)	GFC (0.430g E)	GFF (0.592g E)	FG Tape (0.183g E)
—	- - -	· · ·	- · - ·	- - - -

1.25"-dia. cells used
Flooded anodes.

Figure 5. Performance at 400°C and 62 mA/cm² Steady-State Current Density of Li(Si)/LiCl-KCl/FeS₂ Single Cells made with Various Filter and Tape Separators.

Polarization for Li(Si)/LiCl-KCl/FeS₂ (UL) Cells at 400C & 63 mA/cm² for Various Separators Dipped in Molten Electrolyte



Pressed Powder (0.670g E)	GFA (0.395g E)	GFC (0.430g E)	GFF (0.592g E)	FG Tape (0.183g E)
—	- - -	· · ·	- · - ·	- - - -

1.25"-dia. cells used
Flooded anodes.

Figure 6. Total Polarization at 400°C and 62 mA/cm² Steady-State Current Density of Li(Si)/LiCl-KCl/FeS₂ Single Cells made with Various Filter and Tape Separators.

As mentioned earlier, the degree of electrolyte loading in the separator is important for thermal-cell performance. There is some minimum loading that is necessary for proper functioning of the cell. As the electrolyte loading is increased with conventional pressed-powder separators, there is a corresponding improvement in cell performance. After a certain level, however, the relative electrical performance does not increase further. This effect was not generally seen with the glass-fiber separators. The electrolyte loading will depend on the pore-size distribution of the particular separator material (or MgO powder). This is seen in Table 3 where the active lives of the cells are listed to a 1.25-V cutoff for the various cells tested. A lower electrolyte loading will reduce thermal requirements (heat pellet weight) for batteries.

Table 3. Relative Performance of Li(Si)/LiCl-KCl/FeS₂ Cells at 400°C Under a Steady-State Load of 63 mA/cm².

<u>Separator Material</u>	<u>Avg. Life to 1.25 V, s</u>	<u>Loading of Electrolyte, g*</u>
Fiberglass tape	782	0.183
Whatman GF/A filter	1565	0.395
Whatman GF/C filter	1650	0.474
Whatman GF/F filter	1495	0.601
MgO powder	2045	0.650

* Loading per 1.25"-dia. test disc after immersion in molten salt.

The improvement was dramatic for the GF/A vs. the glass-tape cell due to doubling of the electrolyte present in the separator. However, there wasn't a corresponding improvement for the other separators when the electrolyte loading reached 0.6 g/disc. The best overall performance in terms of active life was still obtained with the standard cell using the MgO separator. However, the upper plateau voltage was greater for the cell with the GF/A separator, although it did not have the extended lower-voltage plateau observed with the control cell. *In the end, the final overall performance will depend on how much of the original electrolyte remains in the separator during discharge.* This, in turn, will depend on the pore-size distribution and electrolyte wettability of the separator—whether glass tape or discs, or MgO powder. During discharge, migration of the electrolyte in the separator can occur to the adjacent anode and cathode pellets, thus resulting in some degree of electrolyte starvation in the separator. There will be competition for the electrolyte to remain in the separator or to wick into the adjoining electrode. The outcome of this process will determine the ultimate cell performance.

Inventek Separators – Tests were next conducted with separator discs manufactured by Inventek. Samples were prepared by both aqueous dipping and by coating with preweighed amounts of powder and then fusing at 400°C for 15 – 30 min. The results of single-cell tests at 500°C and 125 mA/cm²—a common test condition used at Sandia for screening purposes—are summarized in Figure 7. The cells with the Inventek separator provided performance superior to that with the standard pressed-powder separators, even though the total polarization (effective impedance) was slightly higher near the first voltage transition. The upper-voltage plateau was also longer.

Immersion of the separator disc into the aqueous solution resulted in a much greater electrolyte loading than was required (1.35 g) due to the disc being thicker than desired (0.0289” – 0.0362” vs. 0.027” for the cold-pressed separator pellet). However, by using the powder-fusion process, an electrolyte loading of only 0.7 – 0.75 g was readily attained. At this level, the cell still outperformed the control cell as well as the cell with the aqueous-salt-impregnated separator disc under these conditions.

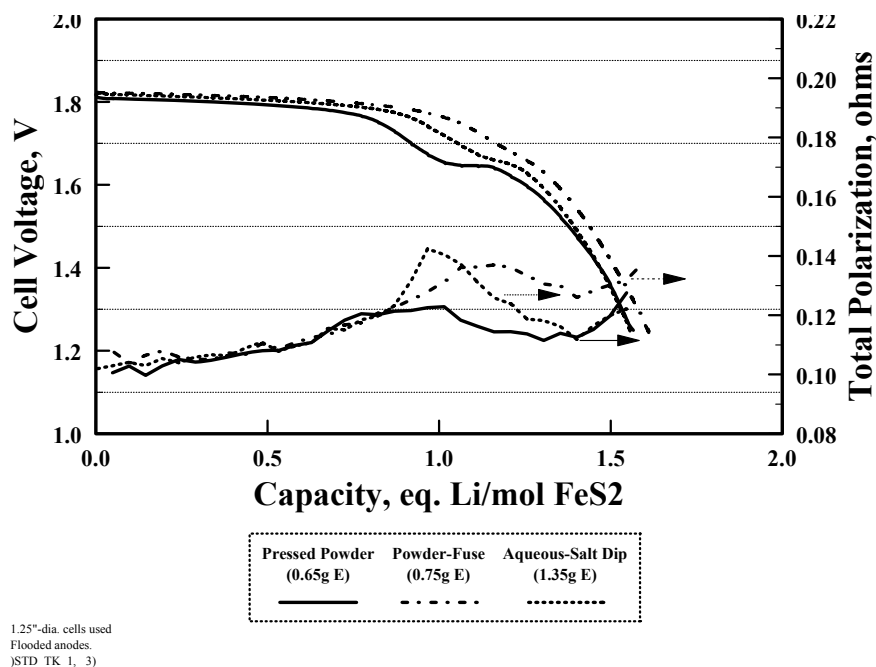


Figure 7. Performance at 500°C and 125 mA/cm² of Li(Si)/LiCl-KCl/FeS₂ Single Cells using Inventek Ceramic Separator Discs.

These Inventek discs were thicker than desired and were used as received for proof of concept of their viability. However, it should be possible to make such discs much thinner and still be competitive with the standard pressed-powder separators. They would not suffer from deformation and extrusion that is typical for the pressed-powder separators under a moderately applied load at battery operating temperatures. This should reduce the possibility of shunting parasitic currents caused by electrolyte leakage as well as mitigating against separator breaching.

Commercialization

The processing steps taken in the preparation of samples for laboratory evaluation need to be scalable to be viable in a commercial thermal battery environment. Once a suitable material has been identified, it should be possible to develop the necessary processes and procedures with appropriate equipment (e.g., moving-belt furnace) to make this approach feasible for large-scale production. There would be intrinsic advantages of this approach, in terms of reduced labor, materials, and equipment costs, since there is no need for expensive pressing dies. These preliminary data would indicate that further work in this area is merited to validate the promise of this technology.

Battery Test

Due to time and resource constraints, it was not possible to do a comprehensive study of battery performance of the most promising candidate separator materials. A 5-cell battery test was performed, however, using GF/F separators dipped in the aqueous LiCl-KCl eutectic solution. The voltage and polarization data for this battery were very similar to those for the control battery made with standard pressed-powder separators (Figure 8). This comparison is made all the more valid by the comparable battery stack temperature profiles (Figure 9). These data show that the use of such ceramic/glass separators can be a viable alternative to the conventional pressed-powder separators.

More battery testing under both hot (74°C) and cold (-54°C) conditions would be desirable with this electrolyte and the Inventek separators. Data at higher current densities would also be useful.

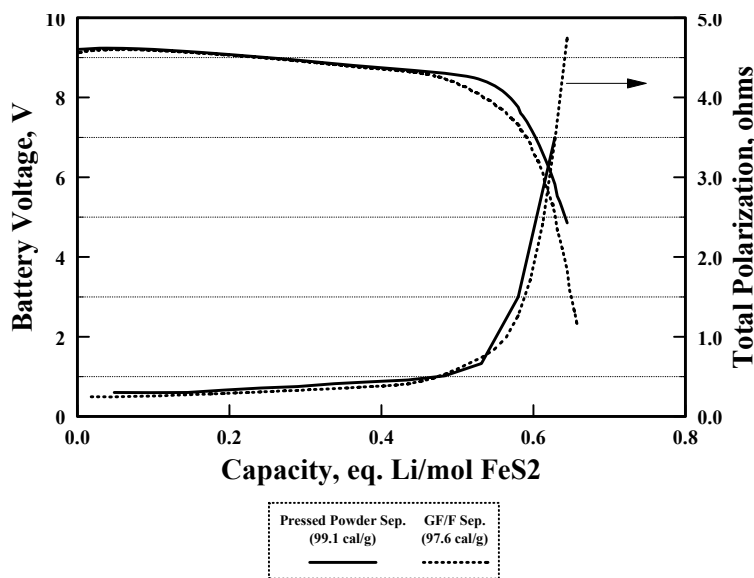


Figure 8. Relative Performance at 125 mA/cm² of 5-Cell Li(Si)/LiCl-KCl/FeS₂ Batteries Activated at -54°C for Pressed-Powder and Ceramic-Fiber Separators.

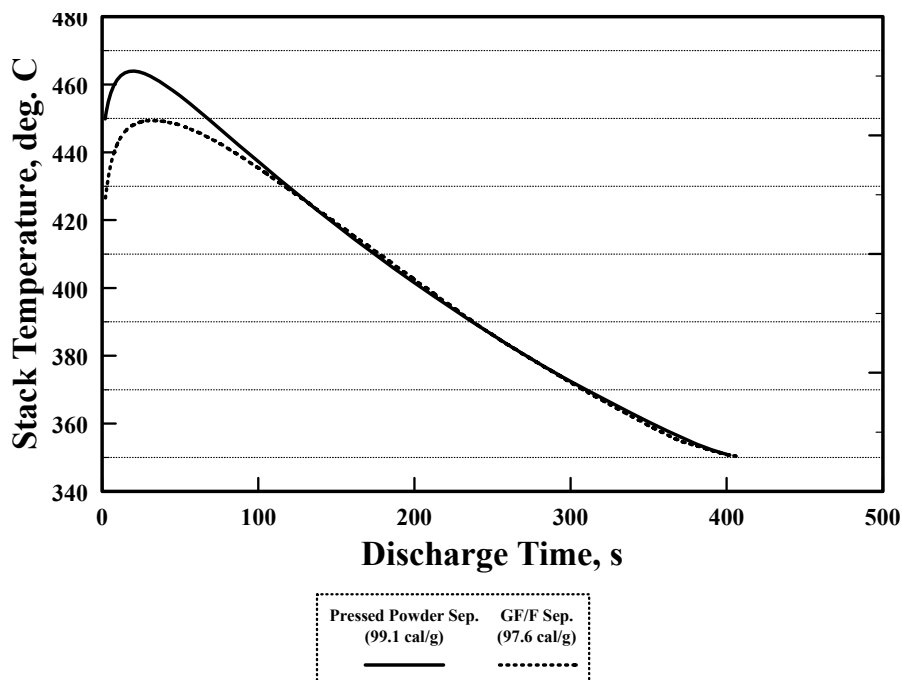


Figure 9. Battery Stack Temperature Profiles for Batteries of Figure 8.

Tests with LiCl-LiBr-LiF Electrolyte

Because of the promising results that were obtained with the separators using the LiCl-KCl eutectic electrolyte, follow-on tests were conducted using the all-Li, LiCl-LiBr-LiF electrolyte. Since this electrolyte melts at a much higher temperature (436°C) than does the LiCl-KCl eutectic (352°C), the immersion temperature was increased from 400° – 450°C to 500°C. This is close to the softening point of the borosilicate glasses. Heat treatment and processing at these elevated temperatures could compromise the performance of these materials, due to devitrification and embrittlement. For this reason, more emphasis was placed on impregnation using a saturated aqueous solution at ambient temperature rather than immersion in the molten electrolyte. The higher melting point required a higher temperature of 500°C for the single-cell tests as well.

Single-Cell Tests

JPS Fiberglass Separator – The voltage response and polarization behavior of single cells with the JPS fiberglass (FG) separators are summarized in Figures 10 and 11, respectively, at 500°C and 125 mA/cm². Data are presented for samples made by dipping in molten LiCl-LiBr-LiF electrolyte as well as those made by dipping in a saturated aqueous solution of the same electrolyte. The electrolyte loading of separator discs dipped in the aqueous solution was ~0.22 g for the as-dipped samples. As expected, prewetting the samples with deionized water first reduced the loading to 0.18 – 0.21 g. These values are 19 – 26% lower than those achieved by direct immersion into the molten electrolyte (~0.27 g). Somewhat higher loadings could possibly be realized by repeated aqueous dippings, however.

The greatest capacities were exhibited by the standard cells made with pressed-powder, MgO-based separators (Figure 10). The performance of the cells with the glass separators was grossly inferior to the control cells. The worst performance was exhibited by cells with separators prepared by aqueous dipping which had lower electrolyte loadings. This reflects the much higher polarizations observed for the cells with the glass separators (Figure 11).

Part of this performance behavior may be related to the relative electrolyte loading. The loadings obtained with the separator discs were only 1/3 of those of the control pressed-powder separator made with MgO. However, the differences in electrolyte loadings for the aqueous-dipped and molten-salt-dipped samples were not that great when one compares the relative performance of the corresponding single cells—over a factor of five in lifetimes. The amount of electrolyte that can be wicked into a separator will depend on the amount of open porosity and the effective relative pore-size distribution. In the case of a woven tape, this will depend on the diameter of the thread and the tightness of the weave (warp and woof). Equally important is the tortuosity of the separator. This determines the effective conduction path and the resulting overall impedance of the separator. This difference is readily evident for the cells with the glass-tape separators.

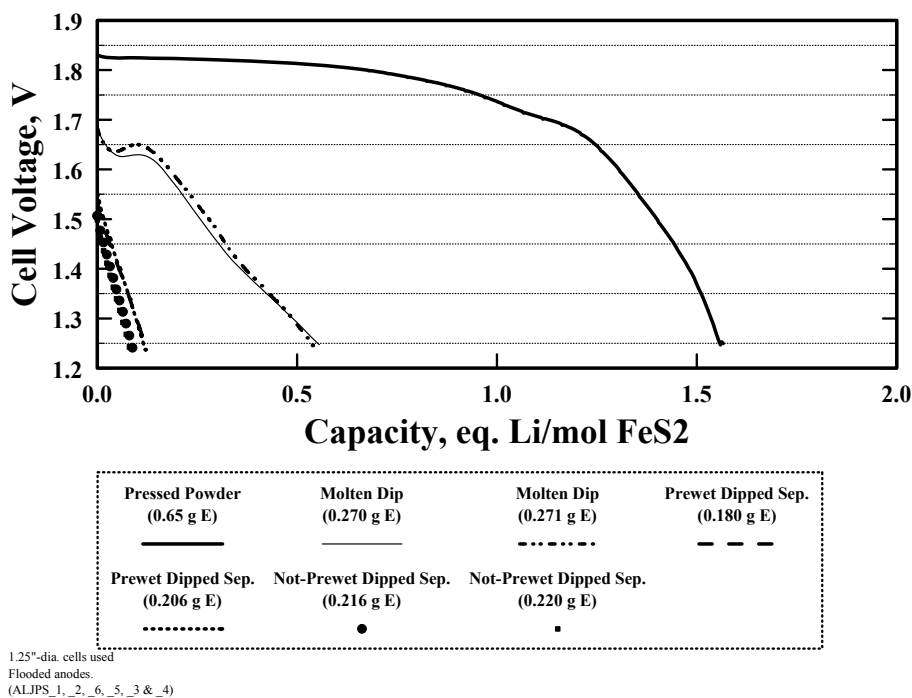


Figure 10. Voltage Response at 500°C and 125 mA/cm² Steady-State Current Density of Li(Si)/LiCl-LiBr-LiF/FeS₂ Single Cells made with JPS Fiberglass-Tape Separator.

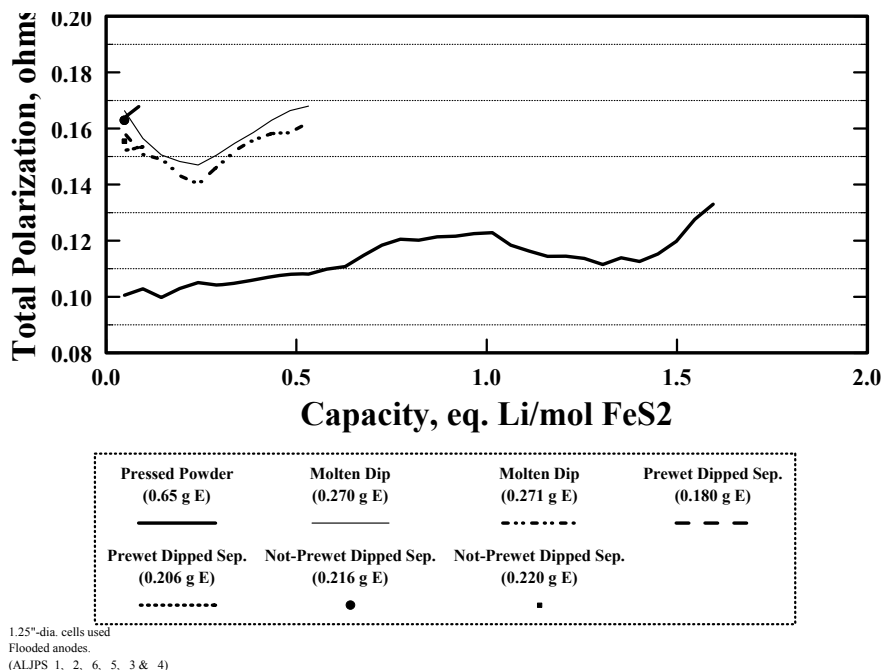


Figure 11. Total Polarization at 500°C and 125 mA/cm² Steady-State Current Density of Li(Si)/LiCl-LiBr-LiF/FeS₂ Single Cells made with JPS Fiberglass-Tape Separator.

GT#1 Fiberglass Separator – A fiberglass tape from Mutual Industries that was thinner than the JPS FG tape was also examined. The results of tests with that material are shown in Figure 12 for discs dipped in molten electrolyte. As expected, this tape had a lower electrolyte loading than the thicker FG tape. The poor performance was comparable to that observed for the JPS FG tape (Figures 10 and 11).

JPS Astroquartz Separator – Another tape product from JPS that was evaluated, Astroquartz, was made of quartz. The electrolyte loadings were slightly higher than those for the FG tapes. The results of tests with this material are summarized in Figures 13 and 14. There was only a slight improvement in performance relative to the FG tapes. The relative trends in performance for the aqueous-dipped and molten-salt dipped samples were comparable to those of the FG counterparts. Neither of these tapes would be suitable for use as separators in thermal batteries.

Zircar ZYW-15 ZrO₂ Tape – Zirconia is much more thermodynamically stable than SiO₂ towards Li(Si) and was evaluated in the form of a woven tape from Zircar. It was very porous (87%) and a higher electrolyte loading was possible with it than for the other tapes examined. This material shows a tendency to be electronically conductive, however, which could interfere with its use as a separator.⁴ The results of single cell tests with this material are summarized in Figures 15 and 16. None of the cells with the tape separators performed as well as the control cell with pressed-powder MgO separators, although the overall performance was much better than for the corresponding cells with the FG or quartz separators. The aqueous-dipped separators outperformed those dipped in the molten electrolyte, which contrasts to what was observed with the FG separators (Figures 10 and 11). However, the molten-salt samples had only half as great an electrolyte loading. The prewet versions did not perform as well as those that had not been prewet, which reflects the much lower electrolyte loading.

Fisher G4 Filter Discs – Separators were prepared for testing using G4 filter discs from Fisher. This material had an unknown pore size and was tested using only the aqueous-dipping procedure. The results of single-cell tests at 500°C are summarized in Figures 17 and 18. The initial voltages for cells with the separators that had not been prewet were higher than those that had been prewet and were comparable to those of the control cells. However, the voltages rapidly dropped during discharge due to the rapid rise in impedance of the separators. The capacities realized were only 1/3 those of the control cells, which was comparable to those observed for cells with the woven-tape separators. The improved initial performance may be due to the much higher electrolyte loadings of ~0.45 g. However, there may be redistribution of the electrolyte into the adjacent anode and cathode during discharge, resulting in starvation of the separator and consequent rapid increase in impedance.

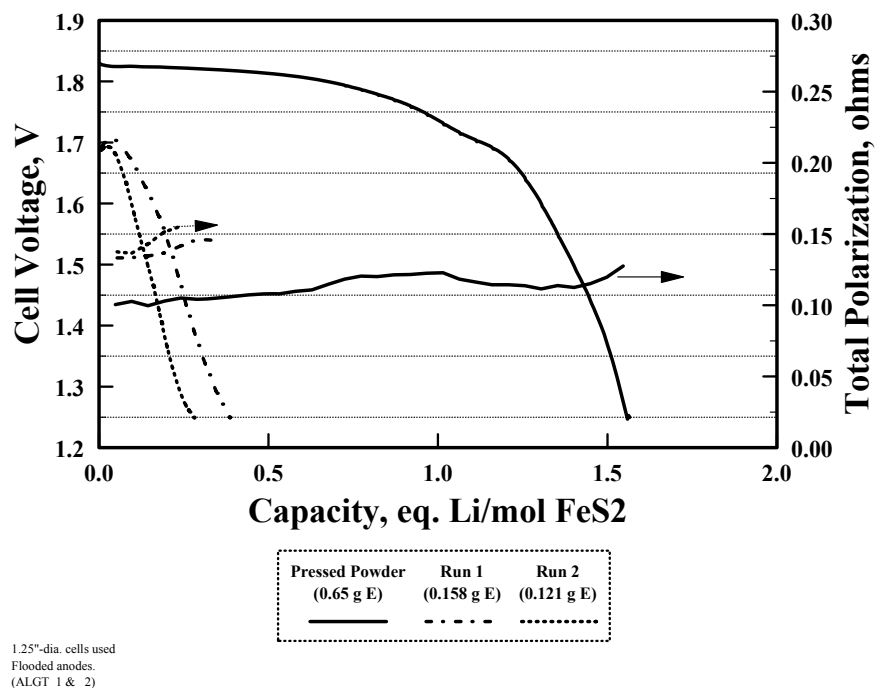


Figure 12. Performance at 500°C and 125 mA/cm² Steady-State Current Density of Li(Si)/LiCl-LiBr-LiF/FeS₂ Single Cells made with Mutual Industries GT#1 Fiberglass-Tape Separator Dipped in Molten Electrolyte.

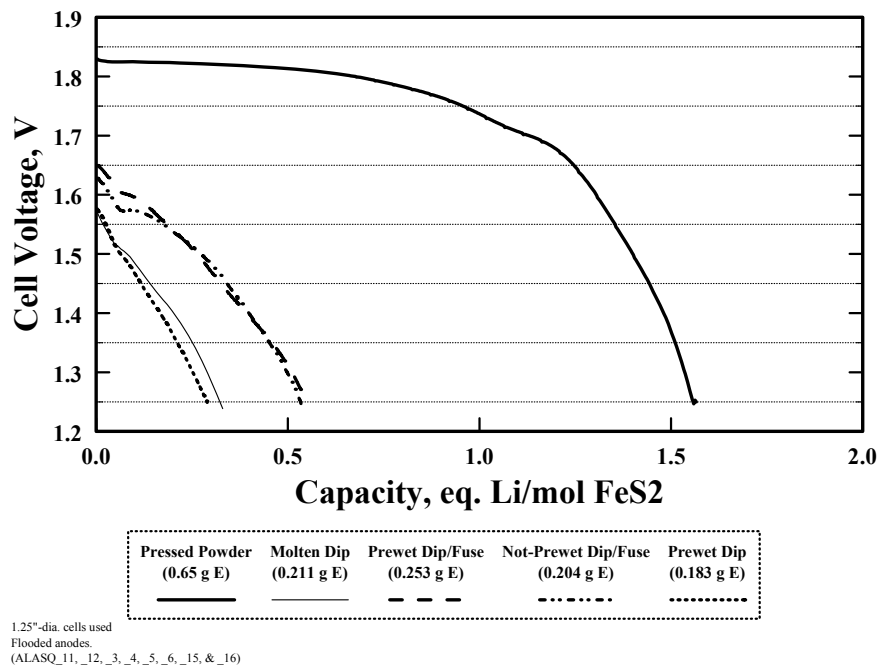


Figure 13. Voltage Response at 500°C and 125 mA/cm² Steady-State Current Density of Li(Si)/LiCl-LiBr-LiF/FeS₂ Single Cells made with JPS Astroquartz Quartz-Tape Separator.

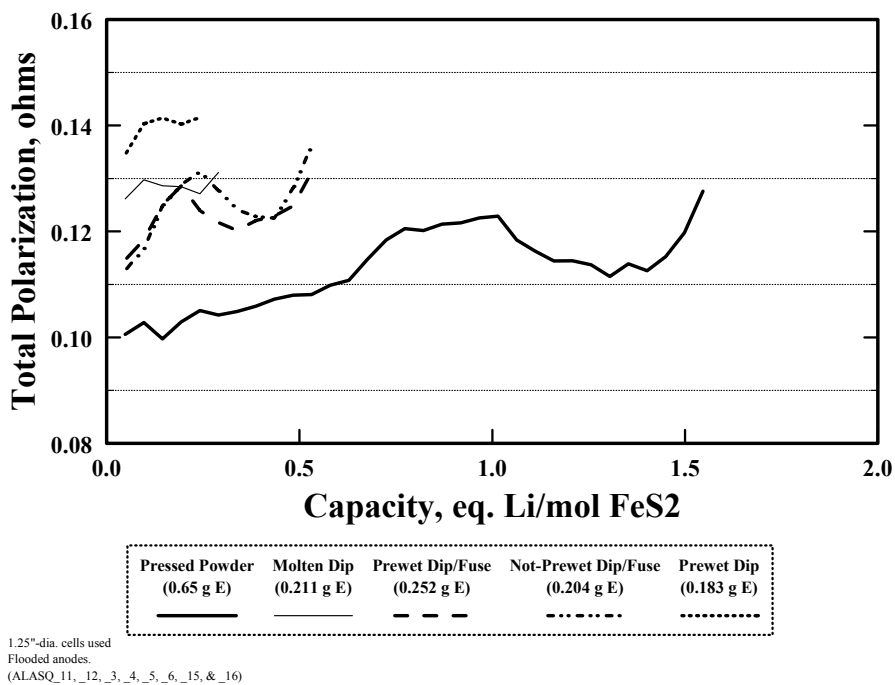
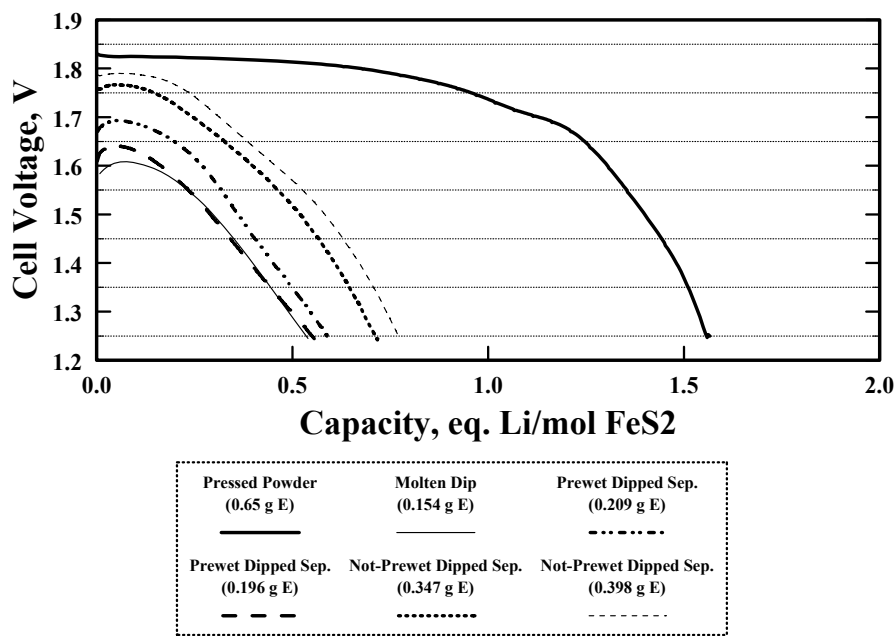
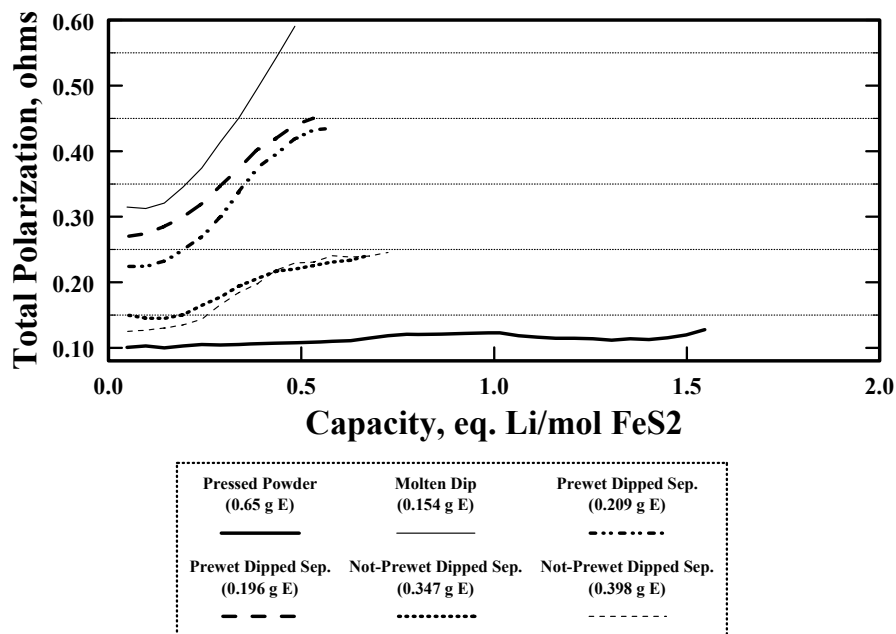


Figure 14. Total Polarization at 500°C and 125 mA/cm² Steady-State Current Density of Li(Si)/LiCl-LiBr-LiF/FeS₂ Single Cells made with JPS Astroquartz Quartz-Tape Separator.



1.25"-dia. cells used
Flooded anodes.
(ALZIR_2_7_6_&_4)

Figure 15. Performance at 500°C and 125 mA/cm² Steady-State Current Density of Li(Si)/LiCl-LiBr-LiF/FeS₂ Single Cells made with Zircar ZYW-15 ZrO₂ Tape Separator.



1.25"-dia. cells used
Flooded anodes.
(ALJPS_1_2_6_5_3_&_4)

Figure 16. Total Polarization at 500°C and 125 mA/cm² Steady-State Current Density of Li(Si)/LiCl-LiBr-LiF/FeS₂ Single Cells made with Zircar ZYW-15 ZrO₂ Tape Separator.

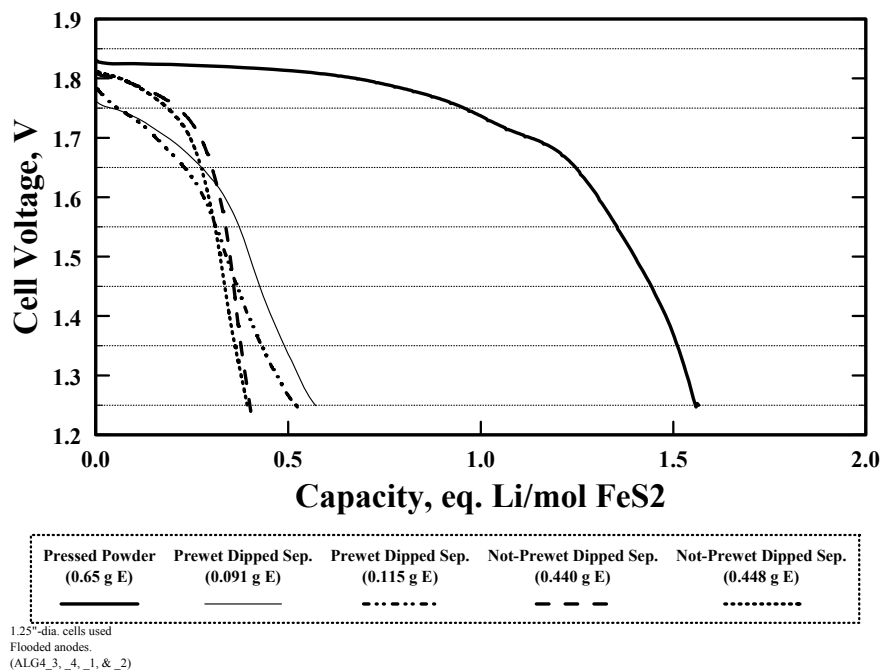


Figure 17. Performance at 500°C and 125 mA/cm² Steady-State Current Density of Li(Si)/LiCl-LiBr-LiF/FeS₂ Single Cells made with Aqueous-Dipped Fisher G4 Filter Separators.

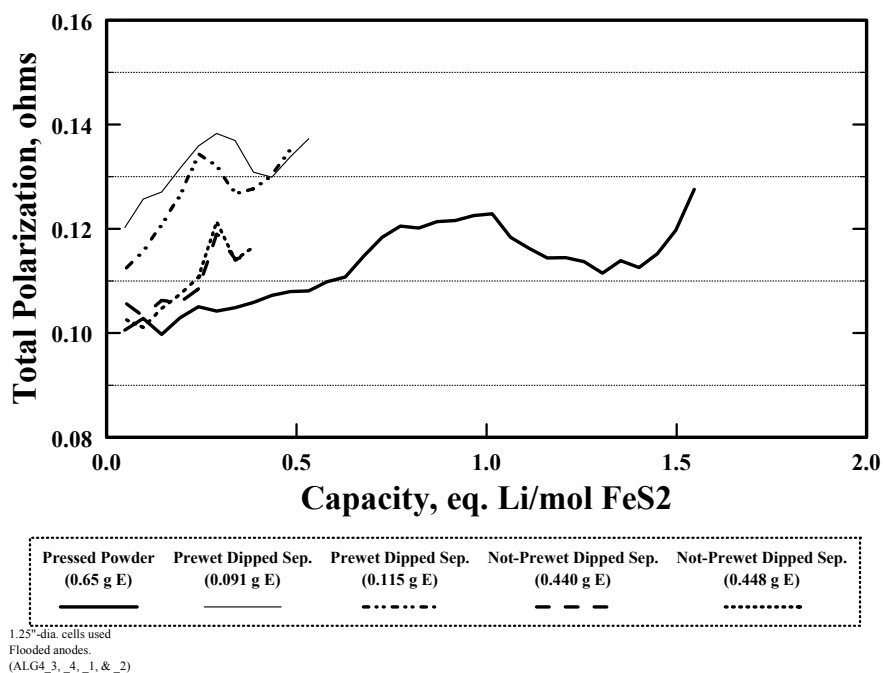


Figure 18. Total Polarization at 500°C and 125 mA/cm² Steady-State Current Density of Li(Si)/LiCl-LiBr-LiF/FeS₂ Single Cells made with Aqueous-Dipped Fisher G4 Filter Separators.

These initial results were not encouraging, so other commercial filter separator materials were examined for possible use as separators for thermal batteries.

Millipore Filter Discs – Millipore manufactures a number of borosilicate filter media with a range in median pore sizes from 0.8 to 1.5 μm . This range provides a possible metric for correlation to the performance when used as separators in thermal cells. The results obtained with the type APFA material, which has the largest median pore size, are summarized in Figures 19 and 20 for aqueous-dipped samples. The initial voltages for cells with the filter separators that had not been prewet were identical to those for the control cells. The voltages were lower for cells where the separators had been prewet and which had only $\frac{1}{2}$ of the electrolyte loading. Unfortunately, the cell voltages dropped rapidly during discharge and approximated those for the cells that used the Fisher G4 filter material. The maximum electrolyte loadings were comparable for the two sets of filters (Fisher and Millipore), which mirrored the observed single-cell performance.

The Millipore type APFC filter has a smaller median pore size than does the APFA—1.2 μm vs. 1.5 μm , respectively. The results of single-cell tests using it as a separator after the aqueous-dipping procedure are summarized in Figures 21 and 22. The performance was somewhat inferior to that observed with the APFA filters that had a slightly larger median pore size, in spite of the somewhat larger electrolyte loading. The results of tests with the type AP20 filter media, which had the smallest median pore size (as low as 0.8 μm), are shown in Figures 23 and 24. Cells with this media showed the worst performance of the three millipore types and had the lowest electrolyte loading. These cells showed even worse performance than did those with the woven-tape separators. The effect of median pore size on the average active lives for the three types of Millipore separators is shown in Figure 25. Cells with untreated discs had about twice the active life as the corresponding Millipore counterpart (APFA), with a somewhat higher electrolyte loading. The performance improved with increase in pore size, but not systematically with electrolyte loading. So, electrolyte loading cannot always be used as a reliable metric for predicting performance under these conditions.

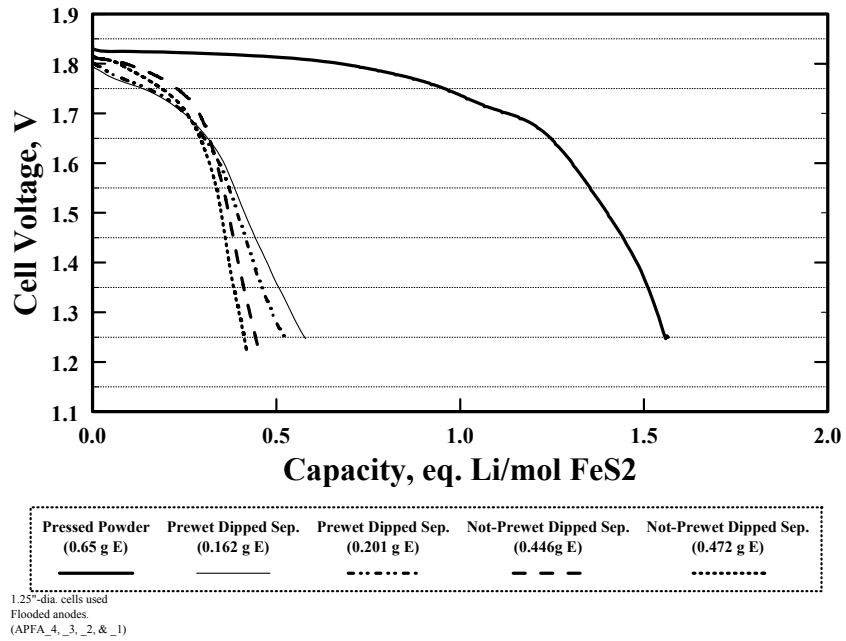


Figure 19. Performance at 500°C and 125 mA/cm² Steady-State Current Density of Li(Si)/LiCl-LiBr-LiF/FeS₂ Single Cells made with Aqueous-Dipped Millipore APFA (1.5 μm) Filter Separators.

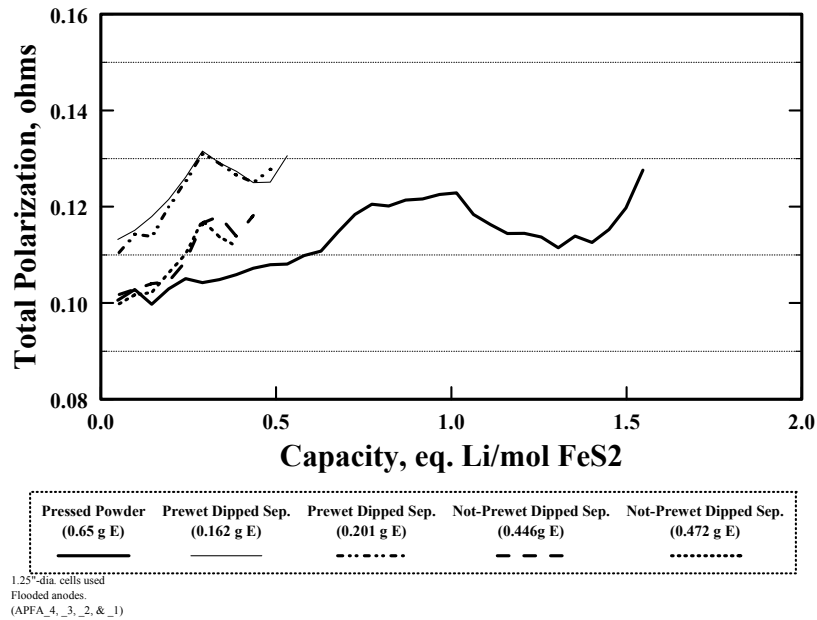


Figure 20. Total Polarization at 500°C and 125 mA/cm² Steady-State Current Density of Li(Si)/LiCl-LiBr-LiF/FeS₂ Single Cells made with Aqueous-Dipped Millipore APFA (1.5 μm) Filter Separators.

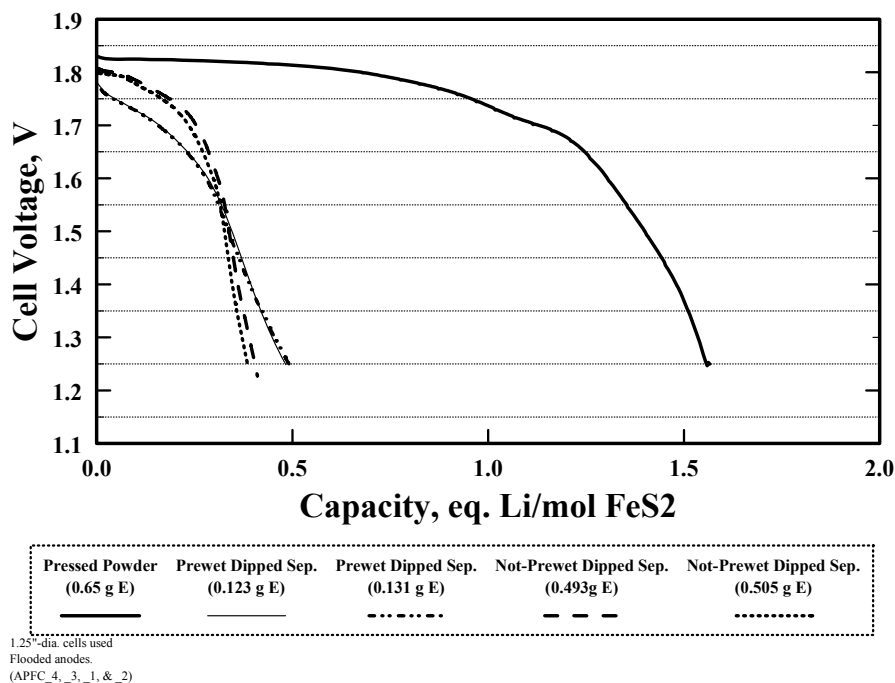


Figure 21. Performance at 500°C and 125 mA/cm² Steady-State Current Density of Li(Si)/LiCl-LiBr-LiF/FeS₂ Single Cells made with Aqueous-Dipped Millipore APFC (1.2 μm) Filter Separators.

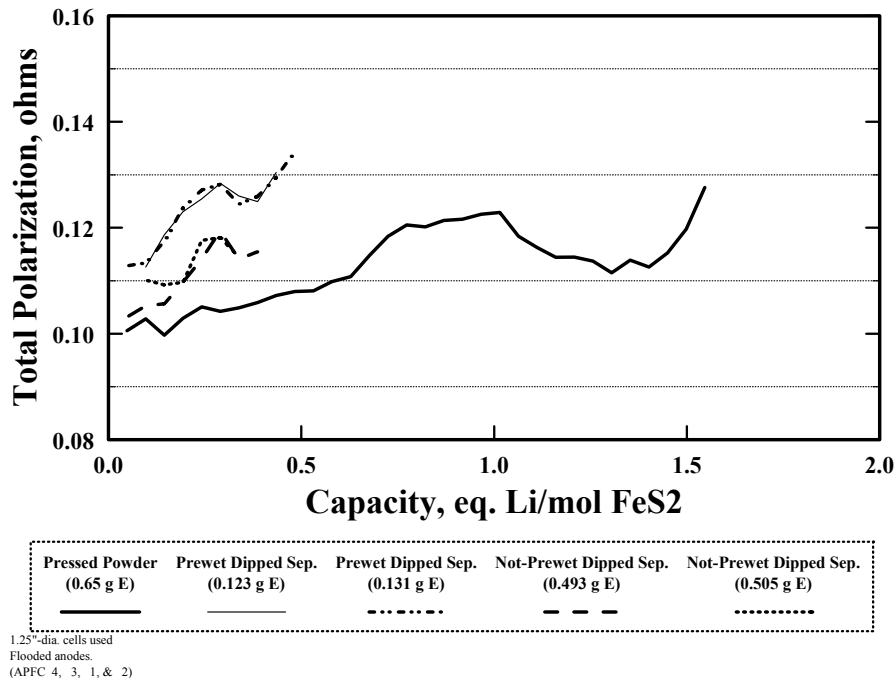


Figure 22. Total Polarization at 500°C and 125 mA/cm² Steady-State Current Density of Li(Si)/LiCl-LiBr-LiF/FeS₂ Single Cells made with Aqueous-Dipped Millipore APFC (1.2 μm) Filter Separators.

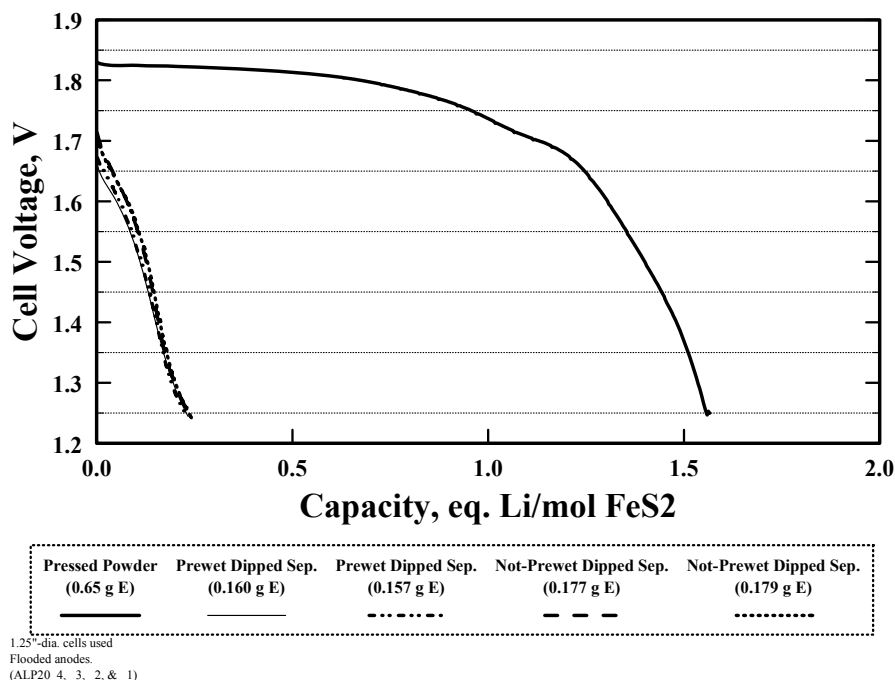


Figure 23. Performance at 500°C and 125 mA/cm² Steady-State Current Density of Li(Si)/LiCl-LiBr-LiF/FeS₂ Single Cells made with Aqueous-Dipped Millipore AP20 (0.8 μm min.) Filter Separators.

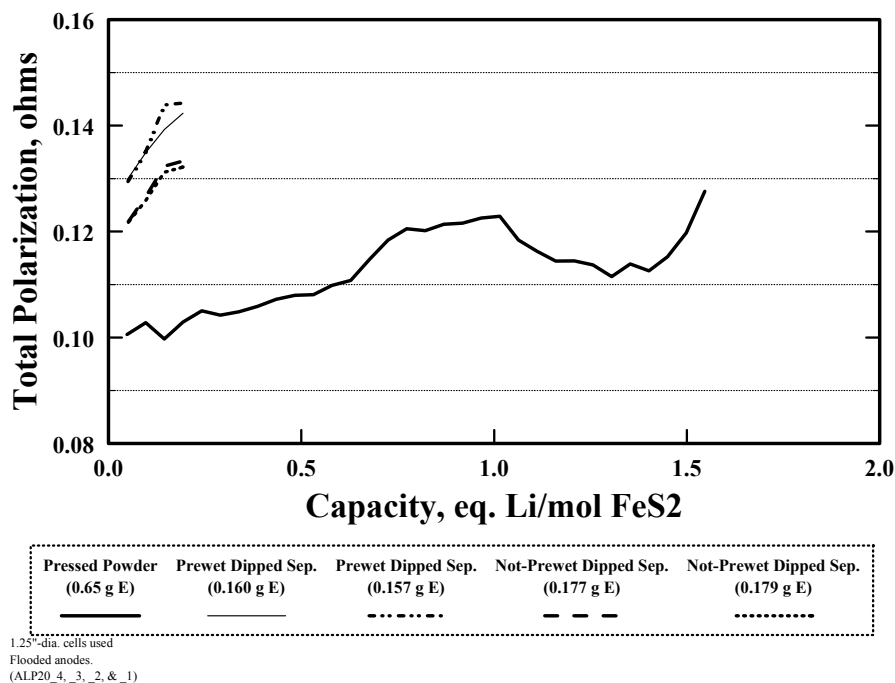


Figure 24. Total Polarization at 500°C and 125 mA/cm² Steady-State Current Density of Li(Si)/LiCl-LiBr-LiF/FeS₂ Single Cells made with Aqueous-Dipped Millipore AP20 (0.8 μm min.) Filter Separators.

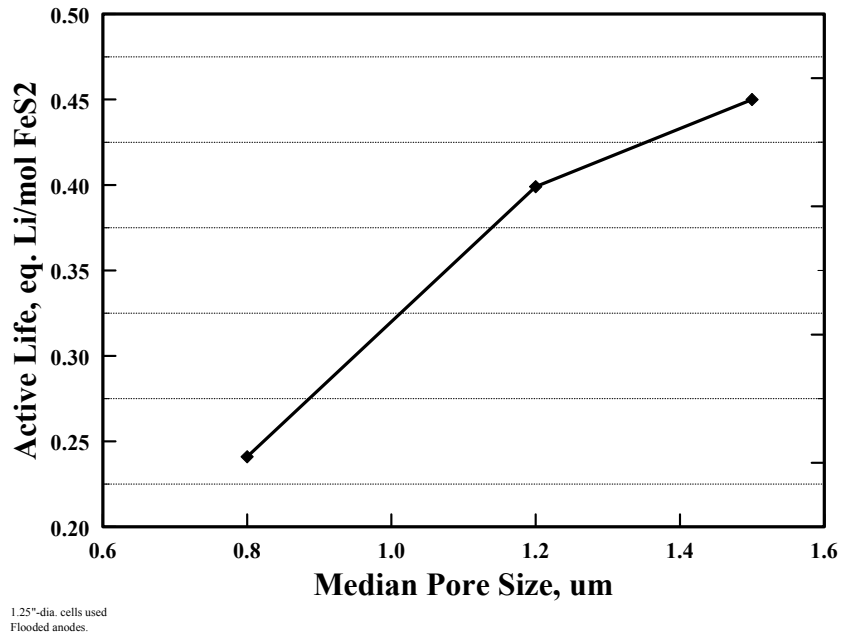


Figure 25. Effect on the Performance at 500°C and 125 mA/cm² Steady-State Current Density of Li(Si)/LiCl-LiBr-LiF/FeS₂ Cells of the Median Pore Size of Millipore Filter Discs used as Separators and Loaded with Electrolyte by Aqueous Dipping.

Whatman Filter Discs – Whatman offers a large variety of borosilicate filter-paper discs in a number of pore sizes, as well as several quartz-based filter media. The results of single-cell tests with type 934-AH media are shown in Figures 26 and 27. (This material has a median pore size similar to that of Millipore APFA.) Prewetting reduced the electrolyte loading to less than 1/3 of that for the untreated samples. Cells with the former separators showed a lower initial voltage that increased during the initial part of the discharge. This indicates improved wetting was occurring during that time. Cells with the untreated, dipped 934-AH separator discs showed initial voltages comparable to those of the control cells, but there was a rapid drop-off after ~0.5 eq. Li/mol FeS₂. The capacities extracted were only ~1/2 of that for the control cells.

The results of tests with the type TCLP material, which has a median pore size of 0.7 μm , are summarized in Figures 28 and 29 for aqueous-dipped samples. There was a dramatic adverse effect on the cell performance when the separators were prewet. The cell polarization was much greater for these samples (Figure 29) which resulted in a rapid decline in discharge voltage (Figure 28). However, the voltages were much lower than those for the control cells and the capacities extracted were only 1/3 as much. This material performed better than the corresponding analogue made by Millipore (*viz.*, AP20), which had only about 1/3 the electrolyte loading. However, the performance of these materials was still unsatisfactory for use as a separator for thermal batteries.

The next series of tests involved the type GF-series of glass-matte filter discs. These materials showed the best overall performance by far of all the commercial materials examined. For these tests, only the GF/C and GF/F versions were used, as they were much more readily wet by the aqueous solutions than was the GF/A material. Initial tests were conducted at 63 mA/cm^2 with the GF/C material and the results are presented in Figures 30 and 31. The cells with the aqueous-dipped separators ran only about half as long as the control cell made with pressed-powder separators.

Coating of the filter discs with electrolyte followed by fusion did not improve cell performance, even at comparable electrolyte loadings. The electrolyte loadings for the filter separators were $1/3$ to $1/4$ as great as that for the control separators. As seen from the data of Table 4, there was no correlation between the lifetimes and the electrolyte loadings.

The effect of prewetting of the separator prior to aqueous dipping was examined at twice the current density. The results of those tests are summarized in Figure 32. Prewetting of the filter discs reduced the electrolyte loading, as expected, and shortened the cell life by half.

Next, the Whatman type GF/F filter material was examined by various treatment techniques. The effects of electrolyte loading for discs immersed in molten electrolyte are shown in Figures 33 and 34. None of the cells with the filter separators performed as well as the control cell, which showed the lowest overall polarization (Figure 34). As the electrolyte loading was increased, the active cell life decreased. This is illustrated in the data of Figure 35. In earlier tests with the LiCl-KCl eutectic electrolyte, the performance of cells tended to improve with the electrolyte loading with similar separator filters. This was not observed when using the all-Li electrolyte, however. The effect of self-discharge could be responsible for the observed behavior. Pyrite has been shown to have a much higher solubility in the all-Li electrolyte relative to the LiCl-KCl eutectic.¹¹ Thus, a higher electrolyte loading would provide a greater reservoir for dissolution of pyrite from the cathode. This, in turn, would consume more pyrite by a self-discharge process, leading to reduced operating life.

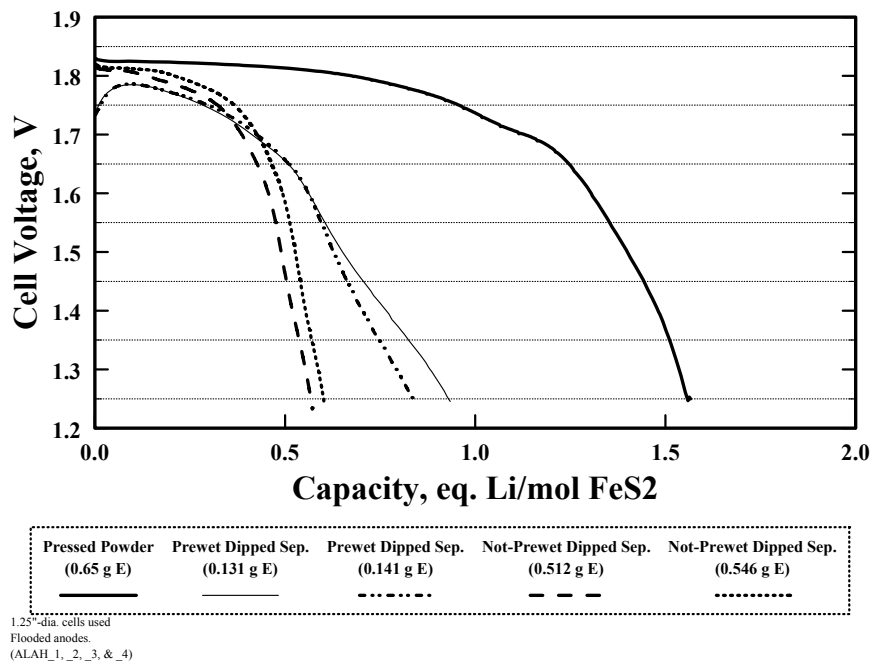


Figure 26. Performance at 500°C and 125 mA/cm² Steady-State Current Density of Li(Si)/LiCl-LiBr-LiF/FeS₂ Single Cells made with Aqueous-Dipped Whatman 934-AH (1.5 μm) Filter Separators.

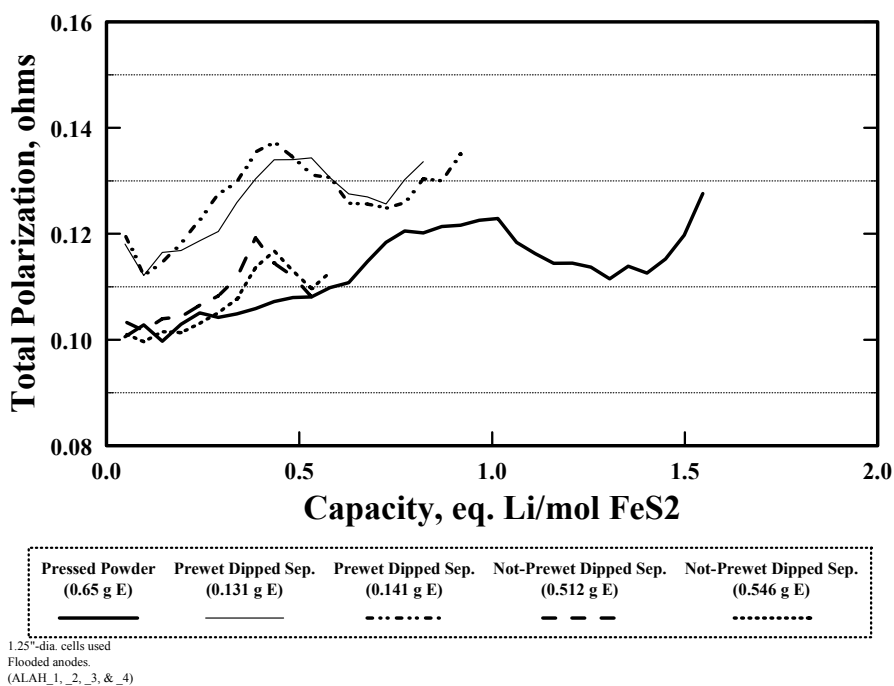


Figure 27. Total Polarization at 500°C and 125 mA/cm² Steady-State Current Density of Li(Si)/LiCl-LiBr-LiF/FeS₂ Single Cells made with Aqueous-Dipped Whatman 934-AH (1.5 μm) Filter Separators.

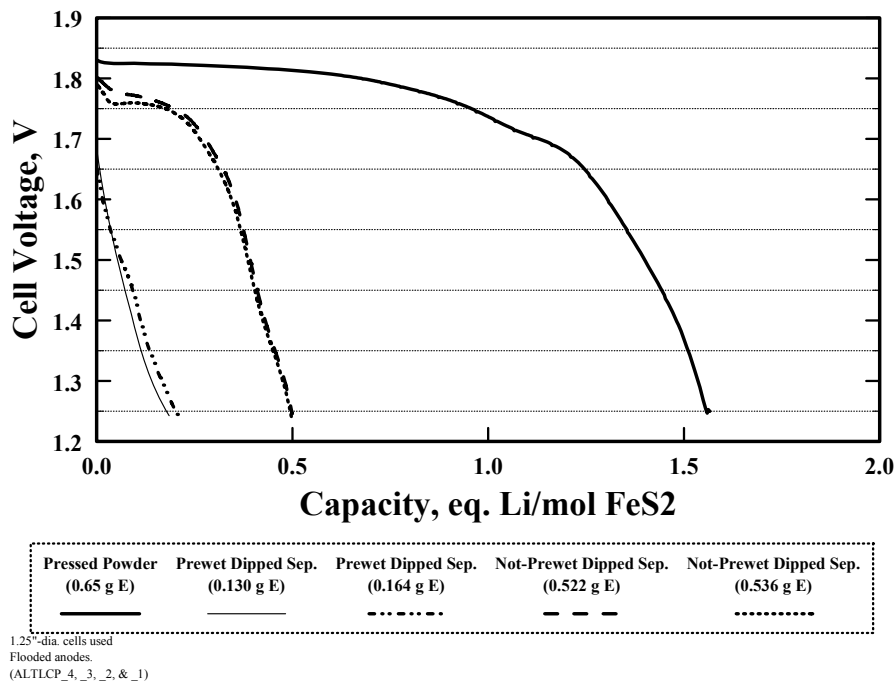


Figure 28. Performance at 500°C and 125 mA/cm² Steady-State Current Density of Li(Si)/LiCl-LiBr-LiF/FeS₂ Single Cells made with Aqueous-Dipped Whatman TCLP (~0.7 μm) Filter Separators.

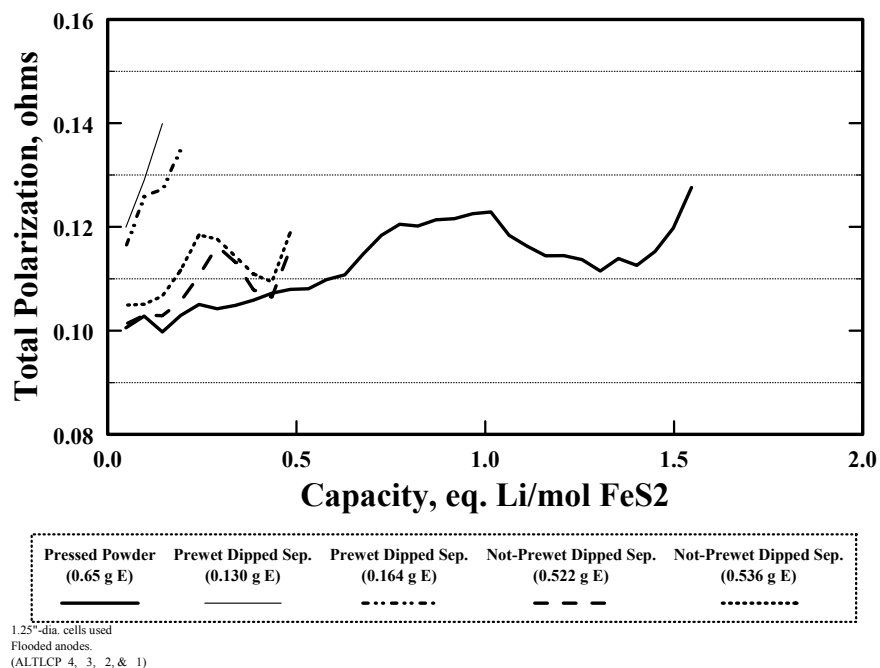
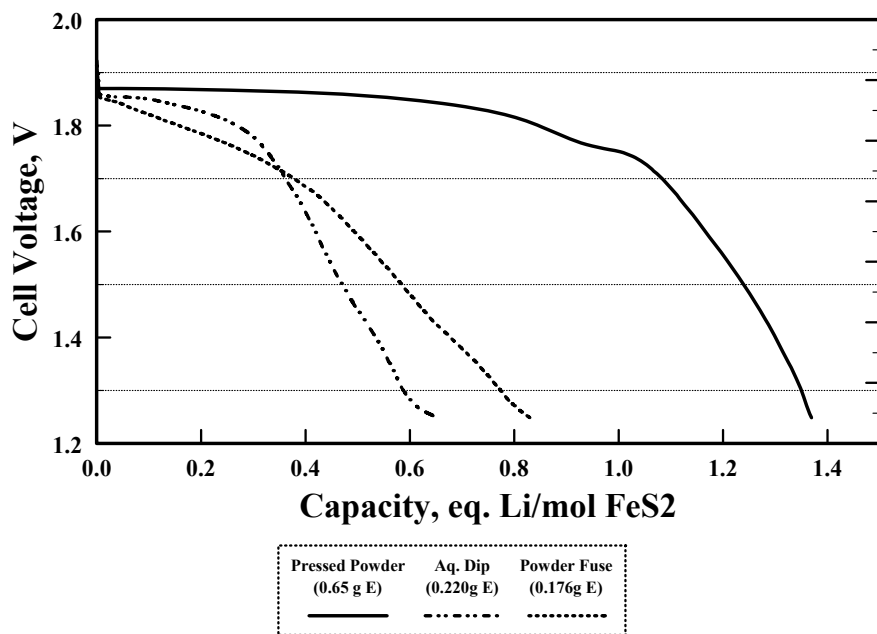
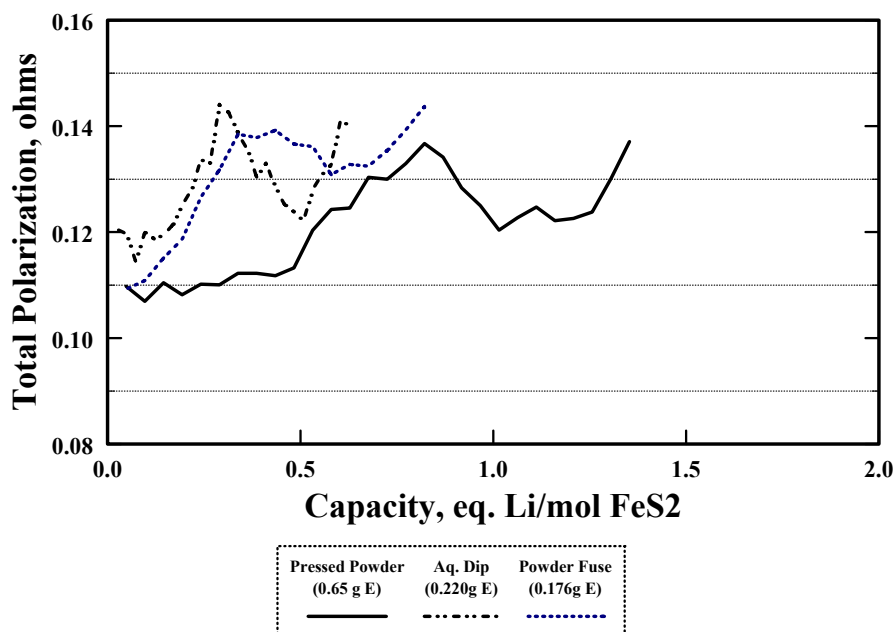


Figure 29. Total Polarization at 500°C and 125 mA/cm² Steady-State Current Density of Li(Si)/LiCl-LiBr-LiF/FeS₂ Single Cells made with Aqueous-Dipped Whatman TCLP (~0.7 μm) Filter Separators.



1.25"-dia. cells used
Flooded anodes.
(CONT_1, ALGFC_1, _2, _5, & _7)

Figure 30. Performance at 500°C and 62 mA/cm² Steady-State Current Density of Li(Si)/LiCl-LiBr-LiF/FeS₂ Single Cells made with Whatman GF/C Treated separators.



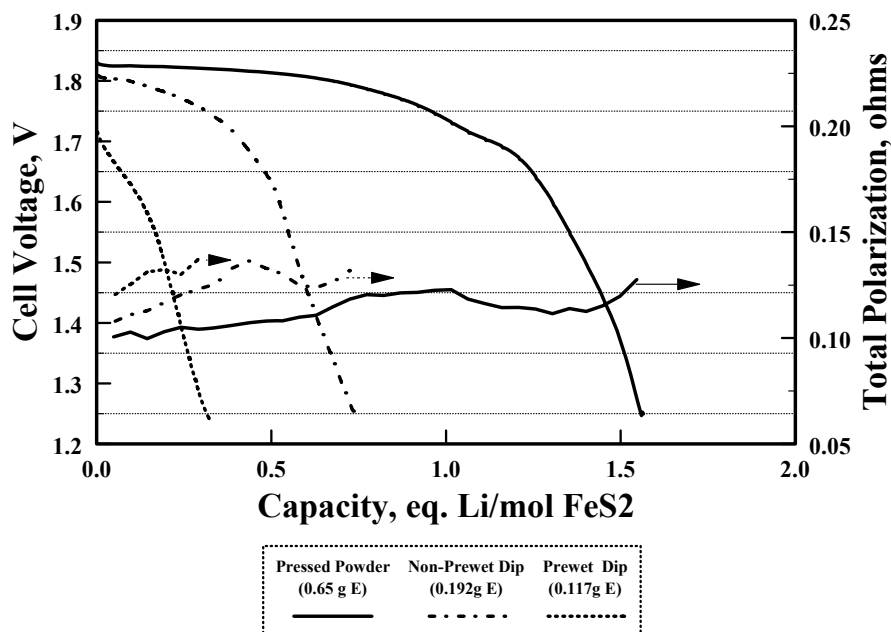
1.25"-dia. cells used
Flooded anodes.
(CONT_1, ALGFC_1, _2, _5, & _7)

Figure 31. Total Polarization at 500°C and 62 mA/cm² Steady-State Current Density of Li(Si)/LiCl-LiBr-LiF/FeS₂ Single Cells made with Whatman GF/C Treated Separators.

Table 4. Relative Performance of Li(Si)/LiCl-LiBr-LiF/FeS₂ Cells at 500°C Under a Steady-State Load of 63 mA/cm² using Whatman GF/C Filter Separators.

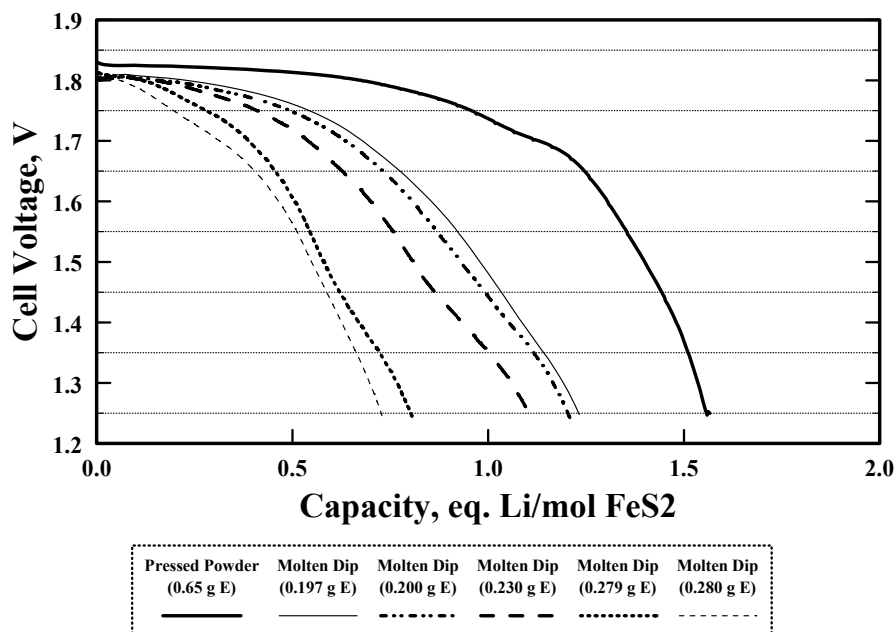
<u>Separator Treatment</u>	<u>Avg. Life to 1.25 V, s</u>	<u>Loading of Electrolyte, g*</u>
Aqueous dip, not prewet	895	0.259
Aqueous dip, not prewet	810	0.220
Aqueous dip, not prewet	1,055	0.139
Aqueous dip, not prewet	890	0.102
Powder coat/fuse	420	0.239
Powder coat/fuse	660	0.189
Powder coat/fuse	515	0.176

* Loading per 1.25"-dia. test disc after immersion in molten salt.



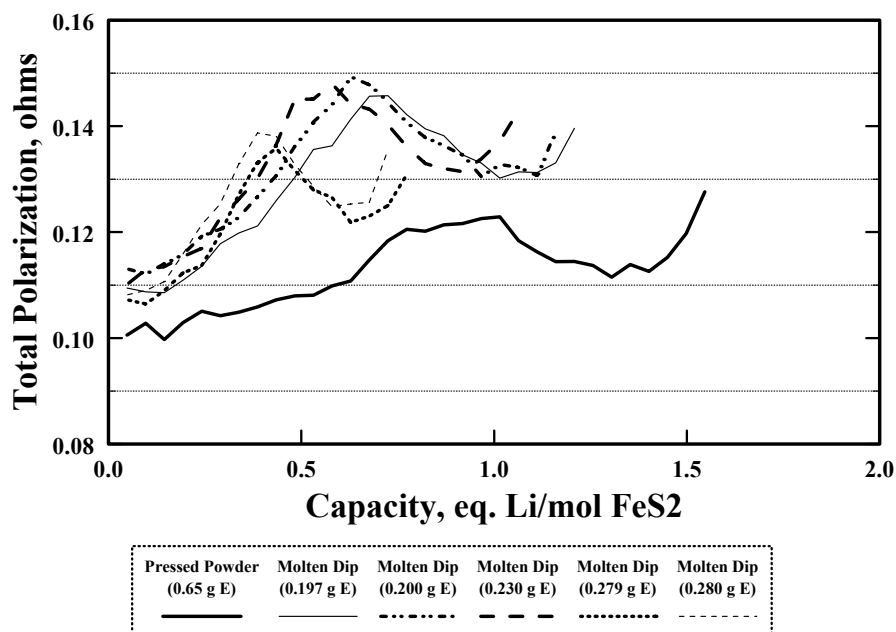
1.25"-dia. cells used
Flooded anodes.
(ALGFC_11, & _13)

Figure 32. Effect of Prewetting of Separator on Performance at 500°C and 125 mA/cm² Steady-State Current Density of Li(Si)/LiCl-LiBr-LiF/FeS₂ Single Cells made with Whatman GF/C Aqueous-Dipped Separators.



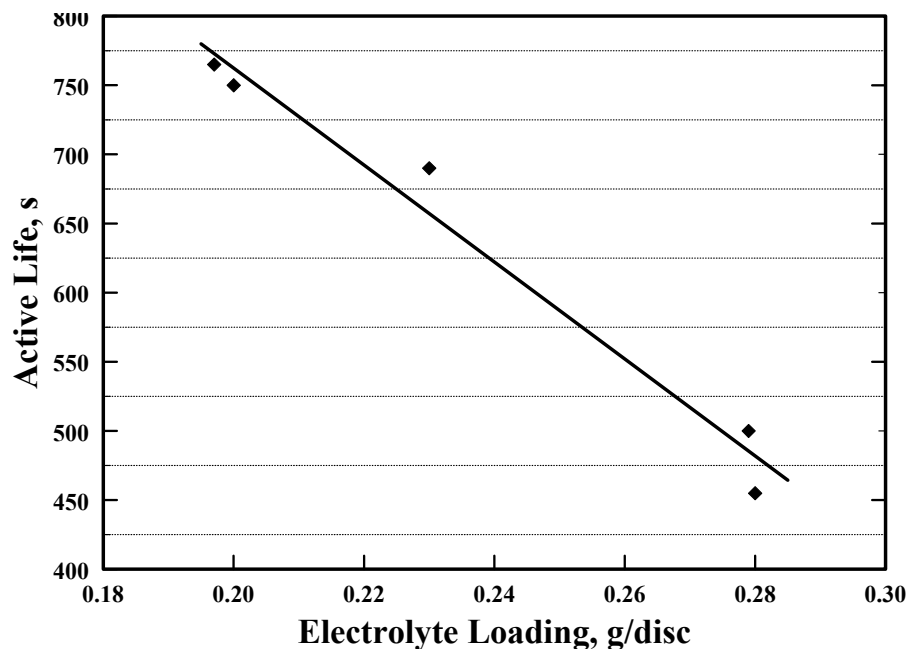
1.25"-dia. cells used
Flooded anodes.
(ALGFF 9_10_11_12_&_13)

Figure 33. Performance at 500°C and 125 mA/cm² Steady-State Current Density of Li(Si)/LiCl-LiBr-LiF/FeS₂ Single Cells made with Whatman GF/F Molten-Salt-Dipped Separators.



1.25"-dia. cells used
Flooded anodes.
(ALGFF 9_10_11_12_&_13)

Figure 34. Total Polarization at 500°C and 125 mA/cm² Steady-State Current Density of Li(Si)/LiCl-LiBr-LiF/FeS₂ Single Cells made with Whatman GF/F Molten-Salt-Dipped Separators.



1.25"-dia. cells used
Flooded anodes.

Figure 35. Effect of Electrolyte Loading of Separator of Li(Si)/LiCl-LiBr-LiF/FeS₂ Cells made with GF/F Impregnated with Molten Electrolyte.

With separator samples prepared by aqueous dipping, higher electrolyte loadings were realized relative to those observed by the molten-salt-dipping procedure. The results of those tests are summarized in Figures 36 and 37 for single dipping, for both as-dipped and prewet separators. The prewetting of the separator reduced the electrolyte loadings by over a factor of three or more. The lower electrolyte loadings resulted in improved performance, with the best results obtained between 0.14 and 0.22 g of electrolyte per separator disc. This corroborates the data for the molten-salt-dipped separators.

The performance under these conditions was the best of all the separator types tried up until this point with the LiCl-LiBr-LiF electrolyte. The separator discs were normally vacuum-dried after the aqueous dipping. Several tests were also done where the discs were fused at 500°C after vacuum drying. The performance in cells was not noticeably affected by this additional heat treatment, so there was no net benefit observed.

The relative performances of the molten-salt-dipped and aqueous-solution-dipped separators under optimum conditions are compared in Figure 38. The cell with the aqueous-dipped separator performed better than that with the molten-salt-dipped separator at comparable electrolyte loadings.

The last Whatman filter type tested was a type QMA material, which is made of quartz instead of borosilicate glass. The cell voltage response at 500°C and 125 mA/cm² in cells made with QMA separators impregnated with the all-Li electrolyte from an aqueous salt solution is summarized in Figures 39 and 40. The overall performance of cells with the QMA separators was very poor, with little difference in performance for the various electrolyte loadings of 0.140 – 0.539 g/disc.

Next, the powder-fusion method for electrolyte loading was used, due to difficulties with wetting by the aqueous solution. The results of single-cell tests with those samples are presented in Figures 41 and 42. The performance of these cells was much improved over those made with aqueous-dipped separators. Electrolyte-loading effects were evident again, with the best results shown by the cell having the separator with the lowest electrolyte loading. This contrasts to the performance observed for the LiCl-KCl eutectic electrolyte (Table 3).

The relative performance of the aqueous-dipped and powder-fusion-treated separators is compared in Figure 43 under optimum conditions. The results for QMA separator were totally unacceptable, relative to those for the GF/F material. The latter was the only commercial material examined that showed some promise when used with the all-Li electrolyte. Very encouraging results were obtained in earlier work with the GF/x materials using the LiCl-KCl eutectic electrolyte. However, those results were not realized when the higher-melting, all-Li electrolyte was substituted for the eutectic electrolyte. Thus, none of these materials would be suitable for use as a separator in thermal cells using the LiCl-LiBr-LiF electrolyte.

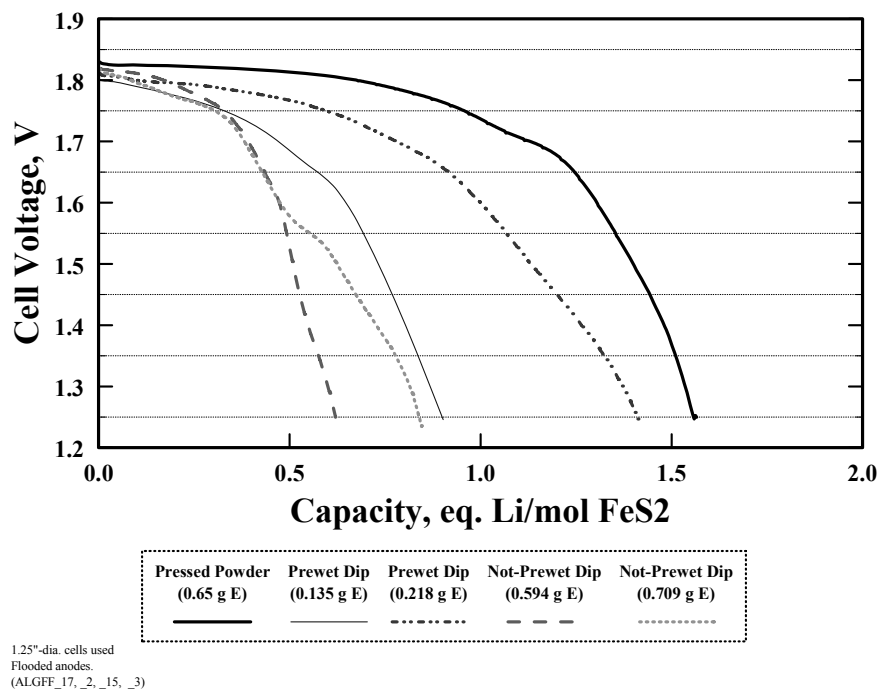


Figure 36. Performance at 500°C and 125 mA/cm² Steady-State Current Density of Li(Si)/LiCl-LiBr-LiF/FeS₂ Single Cells made with Whatman GF/F Aqueous-Dipped Separators.

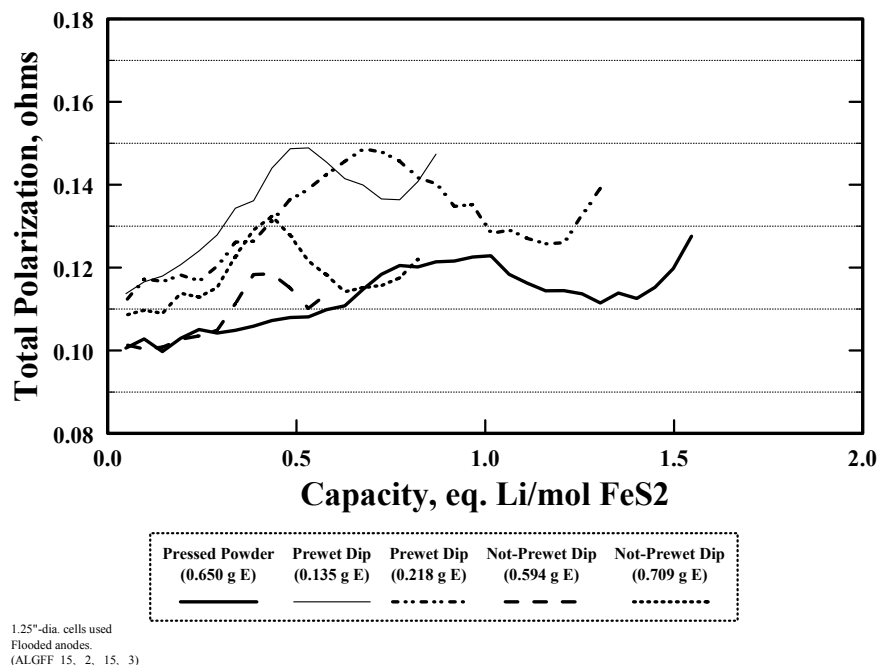


Figure 37. Total Polarization at 500°C and 125 mA/cm² Steady-State Current Density of Li(Si)/LiCl-LiBr-LiF/FeS₂ Single Cells made with Whatman GF/F Aqueous-Dipped Separators.

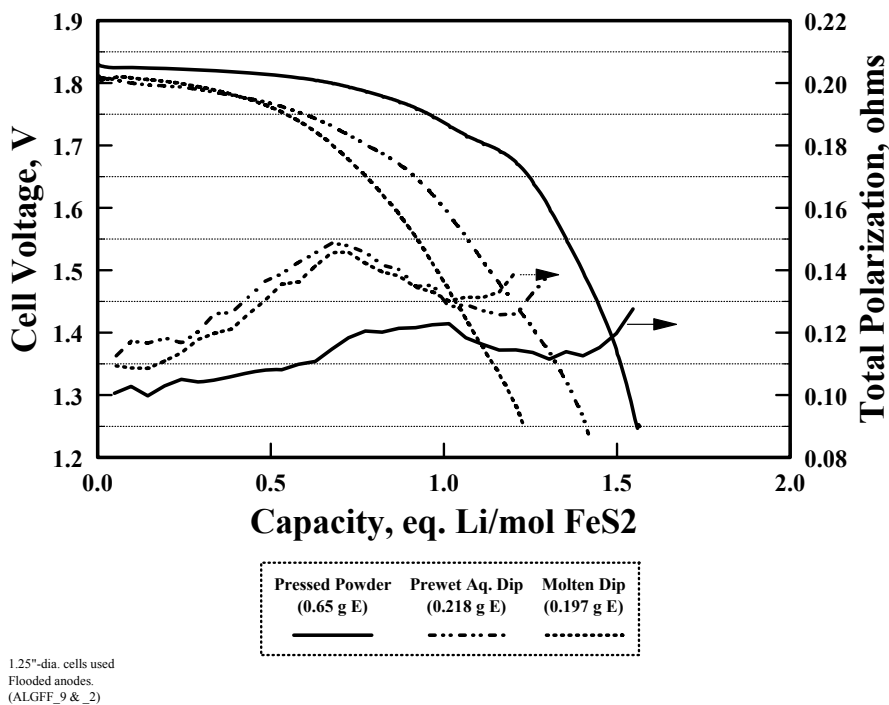


Figure 38. Comparison of Performance of Aqueous-Dipped and Molten-Salt-Dipped Separators at 500°C and 125 mA/cm² Steady-State Current Density in Li(Si)/LiCl-LiBr-LiF/FeS₂ Single Cells made with Whatman GF/F Separators.

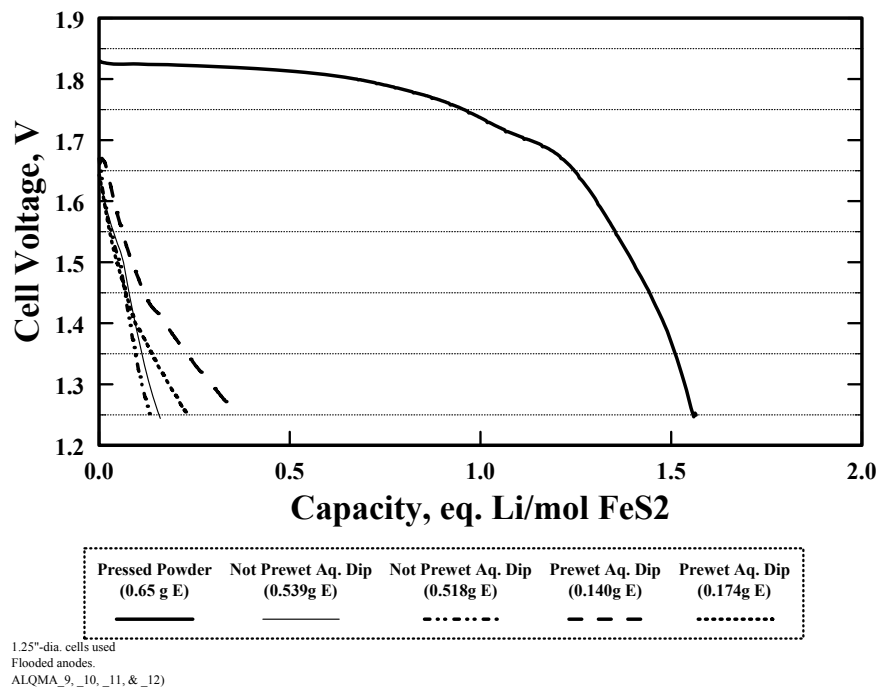


Figure 39. Performance at 500°C and 125 mA/cm² Steady-State Current Density of Li(Si)/LiCl-LiBr-LiF/FeS₂ Single Cells made with Whatman QMA Aqueous-Dipped Separators.

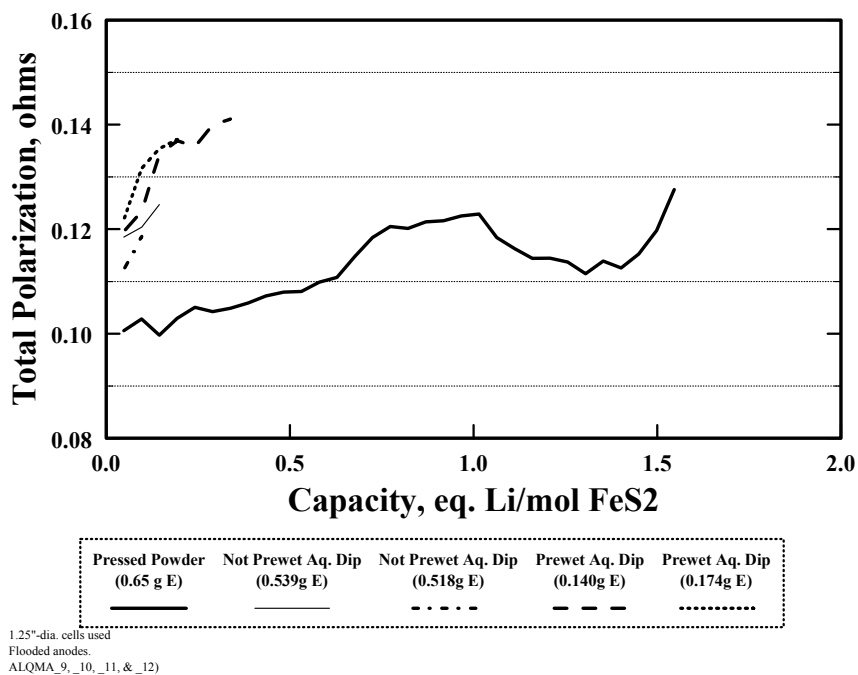


Figure 40. Total Polarization at 500°C and 125 mA/cm² Steady-State Current Density of Li(Si)/LiCl-LiBr-LiF/FeS₂ Single Cells made with Whatman QMA Aqueous-Dipped Separators.

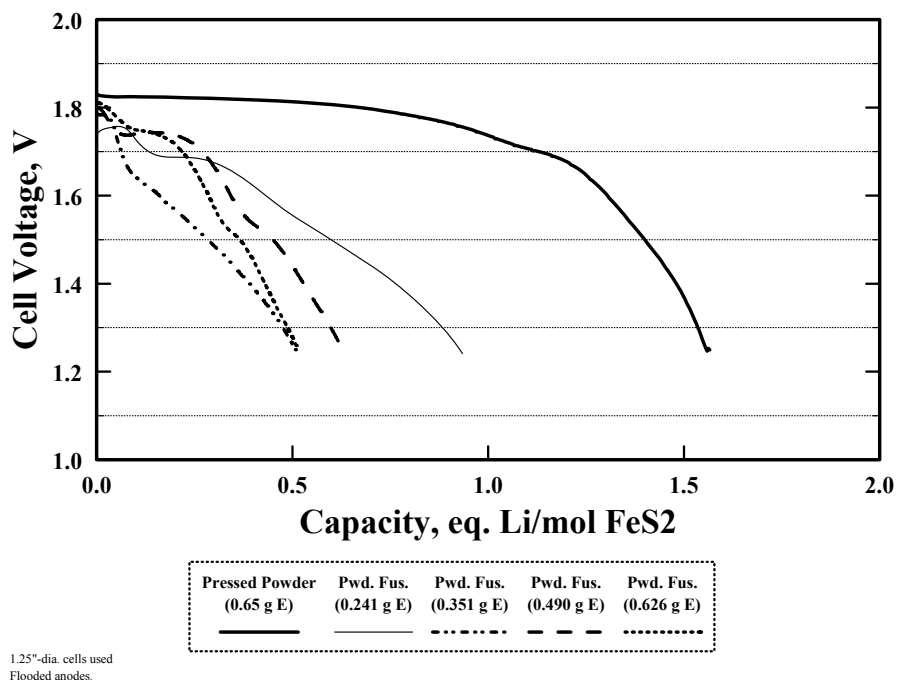


Figure 41. Performance at 500°C and 125 mA/cm² Steady-State Current Density of Li(Si)/LiCl-LiBr-LiF/FeS₂ Single Cells made with Whatman QMA Powder-Fusion Treated Separators.

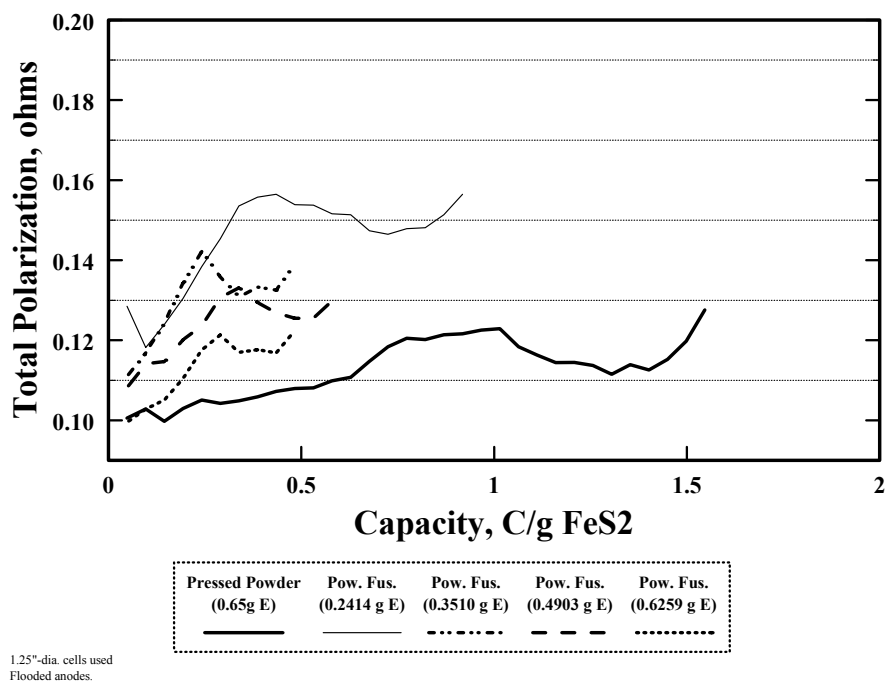


Figure 42. Total Polarization at 500°C and 125 mA/cm² Steady-State Current Density of Li(Si)/LiCl-LiBr-LiF/FeS₂ Single Cells made with Whatman QMA Powder-Fusion Treated Separators.

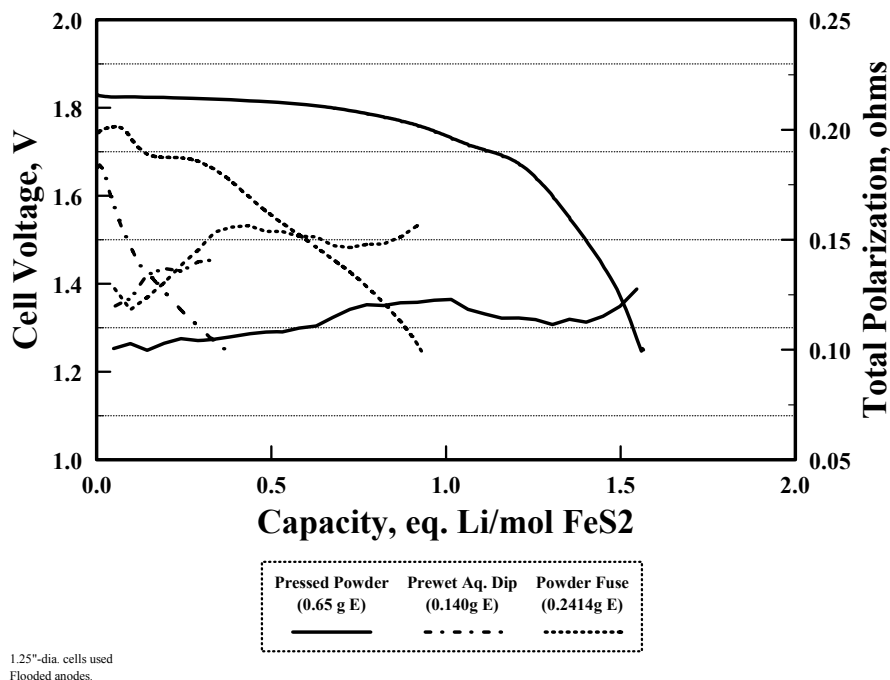


Figure 43. Comparison of Performance of Aqueous-Dipped and Powder-Fusion-Treated Separators at 500°C and 125 mA/cm² Steady-State Current Density in Li(Si)/LiCl-LiBr-LiF/FeS₂ Single Cells made with Whatman QMA Separators.

Inventek Separators – The last candidate separator material that was examined was material that was custom-prepared by Inventek. This material should be more stable at higher temperatures than fiberglass tapes and borosilicate-glass filters. It also should be stable towards devitrification that can occur with quartz filter media. This, coupled with the excellent separator performance observed with the LiCl-KCl eutectic electrolyte (Figure 7) gave rise to high expectations when used with the higher-melting LiCl-LiBr-LiF electrolyte.

The results of single-cell tests at 500°C and 125 mA/cm² with this material in Li(Si)/LiCl-LiBr-LiF/FeS₂ cells are summarized in Figures 44 and 45 for materials treated by the powder-fusion method. There was a noticeable difference in performance between electrolyte loadings of 0.55 g/disc and 0.60 g/disc. At the higher loading, the cell performance was equal to that of the control cell with a pressed-powder separator. This corroborates the good performance observed with the LiCl-KCl eutectic electrolyte and this separator material.

Similar data are presented in Figures 46 and 47 for discs treated by aqueous dipping. The effect of electrolyte loading was dramatic, with cell performance increasing with an increase in electrolyte content. At the highest electrolyte loading of 0.65 g—the same as that for the pressed-powder separator—the experimental cell outperformed the control cell. These results parallel those for separators treated by the powder-fusion method and are extremely encouraging. It should be noted, however, that these results are for only one test condition. Tests should also be conducted at both lower temperatures (*e.g.*, 450°C) and higher temperatures (*e.g.*, 550°C) to validate these initial promising results. Higher current densities should also be examined along with tests in batteries.

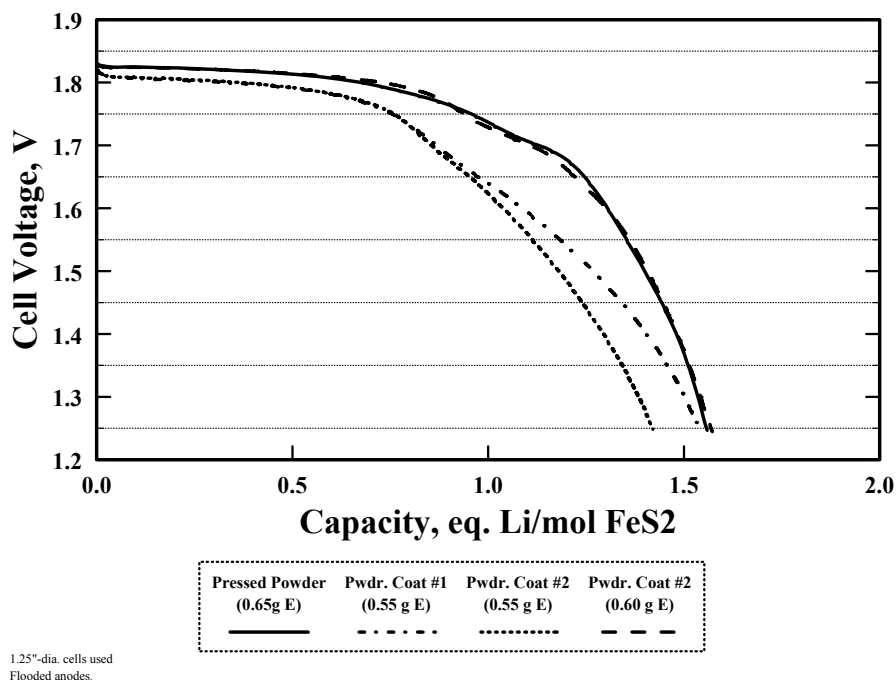


Figure 44. Performance at 500°C and 125 mA/cm² Steady-State Current Density of Li(Si)/LiCl-LiBr-LiF/FeS₂ Single Cells made with Inventek Ceramic-Disc Separators Treated by the Powder-Fusion Method.

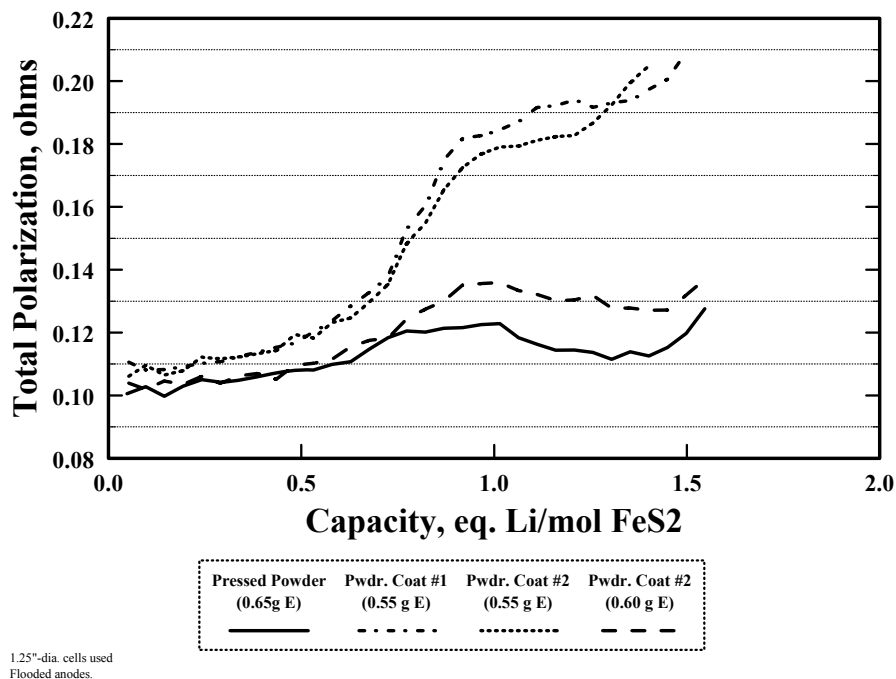
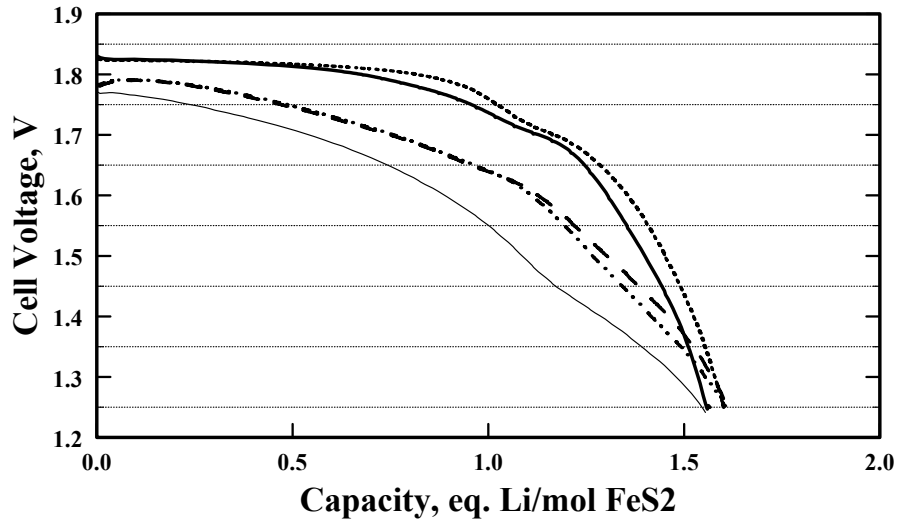


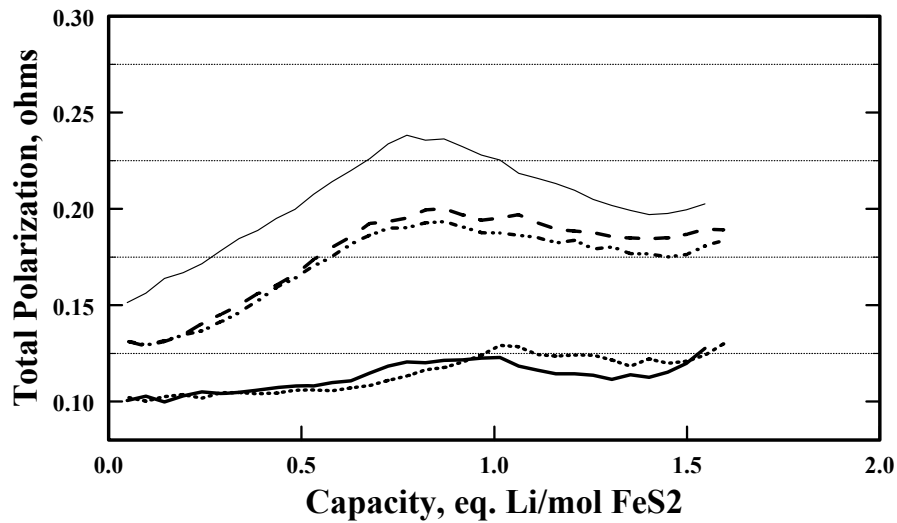
Figure 45. Total Polarization at 500°C and 125 mA/cm² Steady-State Current Density of Li(Si)/LiCl-LiBr-LiF/FeS₂ Single Cells made with Inventek Ceramic-Disc Separators Treated by the Powder-Fusion Method.



1.25"-dia. cells used
Flooded anodes.
(ALTK_2_3_5_&_9)

Pressed Powder (0.65 g E)	Dipped Sep. (0.382 g E)	Dipped Sep. (0.450 g E)	Dipped Sep. (0.480 g E)	Dipped Sep. (C/F#27) (0.650 g E)
—	—	—	—	—

Figure 46. Performance at 500°C and 125 mA/cm² Steady-State Current Density of Li(Si)/LiCl-LiBr-LiF/FeS₂ Single Cells made with Inventek Ceramic-Disc Separators Treated by the Aqueous-Dipping Method.



1.25"-dia. cells used
Flooded anodes.
(ALTK_2_3_5_&_9)

Pressed Powder (0.65g E)	Dipped Sep. (0.382 g E)	Dipped Sep. (0.450 g E)	Dipped Sep. (0.480 g E)	Dipped Sep. (C/F#27) (0.650 g E)
—	—	—	—	—

Figure 47. Total Polarization at 500°C and 125 mA/cm² Steady-State Current Density of Li(Si)/LiCl-LiBr-LiF/FeS₂ Single Cells made with Inventek Ceramic-Disc Separators Treated by the Aqueous-Dipping Method.

CONCLUSIONS

To prepare separator samples, candidate tapes and discs were impregnated by immersion in the molten salt or in saturated aqueous solutions followed by vacuum drying. The best impregnation was obtained by placing preweighed amounts of electrolyte powder on top of the sample discs and then heating them in a furnace above the melting point of the electrolyte to allow it to wick into the pores and spaces between the fibers.

In tests with LiCl-KCl eutectic electrolyte, separators based on the Whatman GF/x borosilicate filter materials ran well in Li(Si)/FeS₂ thermal cells. Cells built with GF/C and GF/F separators ran as well as the control cells with conventional MgO-based, pressed-powder separators when discharged at 400°C and 63 mA/cm². Cells with the GF/A filter performed better than the control cells. The GF/A filter material had the lowest electrolyte loading of the GF/x series when impregnated with molten electrolyte (0.395 g/1.25"-dia. disc). The best results were obtained using the Inventek separators. Cells with the Inventek separator outperformed control cells at 500°C and 125 mA/cm² and comparable electrolyte loadings. More single-cell tests under a wide range of discharge conditions and battery tests are merited for this material, but discs ≤0.015" in thickness would be desirable for the envisioned applications.

Only one test was conducted with a 5-cell battery. The results with GF/F media impregnated with the LiCl-KCl eutectic electrolyte were identical to that for the control battery activated at -54°C and discharged at 125 mA/cm². More tests under other discharge conditions would be desirable.

Less favorable results were obtained in separator tests with the higher-melting LiCl-LiBr-LiF electrolyte relative to the LiCl-KCl eutectic. Poor performance was observed in cells with woven fiberglass tapes at 500°C and 62 – 125 mA/cm². These tended to have lower electrolyte loadings than the filter discs in a matte form. Similar poor results were obtained with fiberglass and quartz tapes. Zirconia tape (Zircar ZYW-15) showed higher electrolyte loadings and improved performance relative to the other tapes tested, but performance was still inferior to the control separator. Similar poor performance was observed with all of the Millipore filter media examined. There was no direct correlation between the reported median pore size of these media and the electrolyte loading.

Of all the commercially available filter discs examined, the GF/x series from Whatman performed the best as thermal-cell separators with the all-Li electrolyte. The GF/F filter worked much better than did the GF/C or GF/A filter media. Cell performance with this separator was almost as good as that of the control cell. Better results were obtained with material dipped in an aqueous solution of the electrolyte. This avoids the thermal degradation that can possibly occur during molten-salt impregnation at high temperatures (*e.g.*, devitrification, loss of porosity, etc.). Performance degraded with higher electrolyte loadings with this material and may be related to enhanced self-discharge reactions caused by more dissolution of the pyrite in the electrolyte. The Whatman quartz QMA performed poorly as a separator, with performance characteristics similar to those of the woven tapes.

As for the case of the LiCl-KCl eutectic electrolyte, the best overall results with the all-Li electrolyte were obtained with the Inventek ceramic separators. When impregnated with electrolyte by the aqueous-dip process or the powder-fusion process, this material provided separator performance equal to or, in some cases, better than that obtained with the conventional pressed-powder MgO-based separators.

Use of such a material would obviate the need for expensive pressing dies. Discs of all sizes could readily be punched from such separator material with inexpensive cutting dies. Such a separator would also provide a rigid mechanical barrier between the anode and cathode to ensure bridging will not occur. This is additional insurance for the prevention of thermal runaway. More work with the Inventek separators and the LiCl-LiBr-LiF electrolyte in single cells is merited at higher temperatures and current densities and in battery tests over a range of discharge conditions.

From a commercialization perspective, the use of such separator technology should not present any major technical difficulties. The powder-fusion process is the preferred impregnation method as it provides the closest control on the degree of electrolyte loading. It should be relatively simple to establish a moving-belt furnace with a powder feeder to load the desired amount of electrolyte into the various-sized discs. This should be more efficient than pressing individual pellets as is now done. This could translate into reducing overall labor and materials costs, once the process conditions are optimized.

REFERENCES

1. R. W. Francis and W. L. Worrell, *J. Electrochem. Soc.*, **123** (3), 430 (1976).
2. Private communication with Nick Shuster, Northrop Grumman (1995).
3. G. Bandyopadhyay, R. B. Swaroop, and J. E. Battles, *J. Electrochem. Soc.*, **128** (10), 2187 (1982).
4. J. P. Mathers, T. W. Olszanski, and J. E. Battles, *J. Electrochem. Soc.*, **124** (8), 1149 (1977).
5. R. A. Sharma, R. A. Murie and E. J. Cairns, *J. Electrochem. Soc.*, **123** (8), 1132 (1976).
6. R. N. Singh, J. T. Dusek, and J. W. Sim, *Ceram. Bull.*, **60** (6), 629 (1981).
7. R. A. Sharma, *J. Electrochem. Soc.*, **57** (12), 1103 (1978).
8. T. Chobanov, D. Künze, and F. Woeffler, *Proc. 17th IECEC*, 548 (1982).
9. T. Chobanov, D. Künze, F. Woeffler, *U.S. Patent 4,447,376*, May 8, 1984.
10. Ronald A. Guidotti and Frederick W. Reinhardt, "Evaluation of Fiber Separators for Use in Thermal Batteries," *Proc. Intern. Symp. on Lithium Batteries, Proc.*, **Vol. 99-25**, 772 (2000).
11. Ronald A. Guidotti and Frederick W. Reinhardt, "Electrolyte Effects in Li(Si)/FeS₂ Thermal Batteries," *Proc. 19th Intern. Power Sources Symp.*, 443 (1995).
12. A. W. Adamson, "Physical Chemistry of Surfaces", 3rd ed., pp. 333 – 371, J. Wiley and Sons, New York (1976).
13. W. D. Kingery, H. K. Bowen, and D. R. Uhlmann, "Introduction to Ceramics", 2nd ed., pp. 137 – 216, J. Wiley and Sons, New York (1976).

UNLIMITED DISTRIBUTION

- 1 Wright Laboratory
Aero Propulsion and Power
Directorate
Attn: D. M. Ryan
WL/POOS-2
1950 Fifth St.
Wright-Paterson AFB, OH
45433-7251
- 1 Inventek.
Attn: T. Kaun
320 Willow St.
New Lenox, IL 60451
- 2 Army Research Lab
Attn: F. Krieger
A. Goldberg
2800 Powder Mill Road
Adelphi, MD. 20783
- 1 A. A. Benderly, Consultant
9915 Logan Dr.
Potomac, Maryland 20854
- 4 Eagle-Picher Technologies, Inc.
Attn: C. Lamb
J. DeGruson
R. Hudson
M. Parrot
P.O. Box 47
Joplin, MO 64802
- 1 Naval Ordnance Station
Attn: K. Englander
Code 5123C
Indian Head, MD 20640
- 3 Naval Surface Warfare Center
Attn: C. Winchester
P. Keller
Dr. Patricia Smith
Code 683, Electrochemistry Branch
9500 McArthur Blvd.
W. Bethesda, MD 20817-5700
- 3 Naval Weapons Center
Attn: R. Nolan (Code 3626)
D. Rosenlof (Code 3626)
Carl Hinnners (Code 477400D)
China Lake, CA 93555
- 3 SAFT America
Attn: K. K. Press
Doug Briscoe
Guy Chagnon
107 Beaver Court
Cockeysville, MD 21030
- 1 D. Benner
PerkinElmer Optoelectronics
1100 Vanguard Blvd.
Miamisburg, OH 45342
- 3 Ron Guidotti
Sierra Nevada Consulting
1536 W. High Pointe Ct.
Minden, NV 89423
- 1 Leclanche, S.A.
Attn: P. Reutschi
48, Avenue de Grandson
CH-1401 Yverdon-Les-Bain
SWITZERLAND
- 2 ASB
Att: John R. Sweeney
Serge Schoeffert, Research Mgr.
Allée Ste Hélène
18000 BOURGES CEDEX
FRANCE

1 MS0613 M. R. Prairie, 2520
1 MS0613 D. H. Doughty, 2521
1 MS0613 F. M. Delnick, 2521
1 MS0613 D. Ingersoll, 2521
1 MS0613 K. E. Waldrip, 2521
1 MS0614 T. A. Aselage, 2522
5 MS0614 H. W. Papenguth, 2522
1 MS0614 N. D. Streeter, 2521
1 MS0614 R. G. Jungst, 2523
1 MS0614 L. Demo, 2523
1 MS0614 J. A. Gilbert, 2523
1 MS0614 F. P. Lasky, 2523
1 MS0614 L. M. Moya, 2523
1 MS1164 P. C. Butler, 5400
2 MS9018 Central Technical Files, 8944
2 MS0899 Technical Library, 4536

